A review of indirect/non-intrusive reduced order modeling of nonlinear geometric structures

Marc Mignolet, Adam Przekop, Stephen Rizzi, S. Michael Spottswood

▶ **To cite this version:**

Marc Mignolet, Adam Przekop, Stephen Rizzi, S. Michael Spottswood. A review of indirect/non-intrusive reduced order modeling of nonlinear geometric structures. Journal of Sound and Vibration, 2013, 332 (10), pp.2437-2460. 10.1016/j.jsv.2012.10.017 . hal-04588344

HAL Id: hal-04588344
https://hal.science/hal-04588344v1

Submitted on 27 May 2024

HAL is a multi-disciplinary open access archive for the deposit and dissemination of scientific research documents, whether they are published or not. The documents may come from teaching and research institutions in France or abroad, or from public or private research centers.

L'archive ouverte pluridisciplinaire **HAL**, est destinée au dépôt et à la diffusion de documents scientifiques de niveau recherche, publiés ou non, émanant des établissements d'enseignement et de recherche français ou étrangers, des laboratoires publics ou privés.

A review of indirect/non-intrusive reduced order modeling of nonlinear geometric structures

Marc P. Mignolet [a,*], Adam Przekop [b], Stephen A. Rizzi [c], S. Michael Spottswood [d]

[a] SEMTE, Faculties of Mechanical and Aerospace Engineering, Arizona State University, Tempe, AZ 85287-6106, USA
[b] Analytical Mechanics Associates, Inc., Hampton, VA 23666, USA
[c] Structural Acoustics Branch, NASA Langley Research Center, Hampton, VA 23681, USA
[d] AFRL/RQSS Structural Sciences Center, Air Force Research Laboratory, Wright Patterson AFB, OH 45433-7402, USA

The paper presents a review of reduced order modeling (ROM) techniques for geometrically nonlinear structures, more specifically of those techniques that are applicable to structural models constructed using commercial finite element software. The form of the ROM governing equations, the estimation of their parameters, and the selection of the basis functions are reviewed in detail and comparisons of predicted displacements and stresses obtained by the ROM and the full order, finite element models are presented. These ROM methods and validations are extended next to multidisciplinary problems in which the structure is subjected to thermal effects or interacts with the aerodynamics/acoustics. These various applications demonstrate the usefulness and appropriateness of ROMs as computationally efficient alternatives to full finite element models for the accurate prediction of the geometrically nonlinear response of the structures considered.

1. Introduction

Fielding a durable, reusable hypersonic cruise vehicle has been a goal of the USAF since the first flight of the X-15 . The difficulty of realizing this goal cannot be overstated. Hypersonic vehicles operate at the intersection of multiple technical disciplines: thermal, structural, and fluid (acoustics and aerodynamic). Hypersonic vehicle structures will experience high-intensity, random loading resulting in nonlinear response [1,2], and will incorporate structural designs that are necessarily lightweight and efficient with little margin. Further, these vehicles will also be fitted with some combination of turbine/rocket/scramjet propulsion systems whose exhaust will impact portions of the vehicle skin, either on external mold lines or on exhaust ducts. As a result, large dynamic pressure loads, approaching 185 dB (reference 20 μPa), and thermal loads will be applied to relatively thin-walled and hot panel structures, potentially leading to significant fluid–thermal–structure coupling and corresponding thermal–mechanical and fatigue design requirements.

The loading arising from high-intensity jet exhaust impingement or turbulent boundary layer effects [3], is random and band-limited . Response to this extreme loading is often *geometrically nonlinear*, with relatively large dynamic strains. High-cycle, or acoustic fatigue can occur when stiffened aircraft structures have resonant, lightly damped and relatively low-frequency [4] modes within the excitation bandwidth [5]. Acoustic fatigue has consistently plagued jet aircraft of all varieties for the past 50 years or so, and will be a design concern for present and future aircraft [6]. Industry methods, used to design or account for

* Corresponding author.
E-mail address: marc.mignolet@asu.edu (M.P. Mignolet).

Nomenclature

a_i, $a_{d,i}$ component i of the arbitrary vectors $\boldsymbol{a}$ and $\boldsymbol{a}_d$
A_{ij} ij element of an arbitrary matrix $\boldsymbol{A}$
$q_n(t)$, $q_{b,n}(t)$ components n of the generalized coordinates of the reduced order model and of its bending mode-only counterpart
$\mathbf{u}(\mathbf{X},t)$ 3-Component displacement vector at time t of the point of undeformed coordinates $\mathbf{X}$, continuous structure
$\mathbf{y}(t)$, $\mathbf{y}_b(t)$, $\mathbf{y}_m(t)$ displacement vectors of the finite element nodes, total, and bending and membrane components, respectively
$\boldsymbol{\varphi}_b^{(n)}$, $\boldsymbol{\varphi}_m^{(n)}$ bending and membrane displacements basis functions n of the reduced order model for the finite element model
$\boldsymbol{\psi}^{(n)}(\mathbf{X})$, $\boldsymbol{\varphi}^{(n)}$ basis functions n of the reduced order model for the continuous structure and its finite element counterpart

In the list below, A denotes any of the parameters M_{ij}, D_{ij}, $K_{ij}^{(1)}$, $K_{ijl}^{(2)}$, $K_{ijlp}^{(3)}$, F_i as appropriate

A parameters of a reduced order model in which all displacements are modeled
$\overline{A}$ parameters of the reduced order model for the prediction of the bending displacements only
$\hat{A}$ parameters of the finite element model
$\hat{A}_b$, $\hat{A}_m$, $\hat{A}_{bm}$ and $\hat{A}_{mb}$ bending, membrane, and bending–membrane coupling parameters of the finite element model
$\tilde{A}_b$ parameters of the finite element model equations after condensation of the membrane displacements on the bending ones

acoustic fatigue, rely principally on a variety of analytical and empirical techniques [4,7,8]. As vehicle performance envelopes expand, these empirical models will break down, leading to either overly-conservative, heavy designs or, worse, under-designed elements. In recent years the F/A-18 lower nacelle skin [9] and B-2 exhaust-washed aft deck [10] have each suffered from propulsion-load induced sonic fatigue. Considerable attention has been brought to bear on the acoustic fatigue issue, with vast resources spent to develop complex testing facilities, conduct experimental programs, and to produce exhaustive reports and design guides. While the issue has never been a principal design driver, sonic fatigue has cost the aerospace industry enormous amounts of time and resources to retrofit and repair military and civilian aircraft. As the USAF further develops low-observable aircraft and continues to pursue a reusable hypersonic vehicle, sonic fatigue will become a principal design issue. Modern computational tools such as finite element methods and computational fluid dynamics techniques, referred to here as "full order" methods, can of course be used for fatigue prediction. However, the computational cost associated with that effort will be extremely large owing to the very long records to be simulated, the size of each model, the consideration of geometrically nonlinear effects, and the need to fully couple the structural, aerodynamic, and thermal analyses. In fact, the development of such a coupled analysis capability already represents a very significant task [11–13].

The computational challenges described above in connection with hypersonic aircraft are also encountered in many other aerospace and mechanical engineering applications including wings, fan blades, and other thin walled structures in which the loading is large enough to induce geometrically nonlinear effects. Thus, the methods reviewed here may also be applied to these structural applications, as demonstrated for wings [14], a "ballute" [15], and a cylindrical shell [16].

2. Focus and plan

The computational cost and complexity issues associated with the consideration of geometrically nonlinear effects have motivated the formulation and validation of extensions of the modal methods used in linear problems. In such extensions, the displacement components u_i at a point $\mathbf{X}$ of the structure and at time t will be expressed as the expansion

$$u_i(\mathbf{X},t) = \sum_{n=1}^{M} q_n(t)\, \psi_i^{(n)}(\mathbf{X}), \quad i = 1, 2, 3, \tag{1}$$

where $\psi_i^{(n)}(\mathbf{X})$ are specified, constant basis functions and $q_n(t)$ are the time dependent generalized coordinates. Two key elements that complement Eq. (1) and collectively form the reduced order models considered here are as follows:

(i) a strategy to select the basis functions $\psi_i^{(n)}(\mathbf{X})$ and
(ii) a set of governing equations (2nd-order ordinary differential equations) for the generalized coordinates $q_n(t)$.

With regard to the latter element, the present focus is on *parametric* reduced order models, i.e. in which the governing equations have a specific form with coefficients determined for each specific problem. Then, the requirement (ii) is subdivided into the following:

(iia) the determination of the parametric form of the governing equations and
(iib) the identification of the parameters of these equations for a particular problem.

Further, the present review concentrates on *finite element based structural models*, moreover that can be developed on *commercial finite element software* (Nastran and Abaqus have typically been used). Excellent work has clearly been carried out outside of this narrow focus but will not be described here more than the brief discussion of Section 4.1. Finally, only the nonlinearity present in the stiffness operator is considered, i.e. a linear damping model is assumed throughout, as are linear elastic material properties.

The past and present work on the three aspects (i), (iia), and (iib) is reviewed below and a summary of the validation studies and applications carried out is provided. In this regard, it must be recognized that computational speed is only one of the advantages of reduced order models. The ease with which structural computations can be coupled with other disciplinary analyses, e.g. acoustics, aerodynamics, heat conduction, is also a significant benefit of reduced order models.

The derivation of the parametric form of the governing equations for the generalized coordinates (issue (iia) above) is addressed in the next section to provide a foundation for the ensuing developments and validations. Then, a general class of approaches for the identification of the parameters of the governing equations (issue (iib) above, see Section 4) and the selection of the basis (issue (i) above, see Section 5), based on the availability of a finite element model of the structure, are then presented. A sample of validation examples of these latter methods are given in Section 6 while multidisciplinary applications and extensions of the approaches are reviewed in Section 7.

3. Parametric form of nonlinear reduced order models

3.1. General derivation

A general derivation of linear modal models is classically carried out from linear (infinitesimal) elasticity and it is thus desired here to proceed similarly but with finite deformation elasticity to include the full nonlinear geometric effects. Then, the first issue to be addressed is in what configuration, deformed or undeformed, the governing equations ought to be written. In this regard, note that the basis functions $\psi_i^{(n)}(\mathbf{X})$ are expected to (a) be independent of time and (b) satisfy the boundary conditions (at least the geometric or Dirichlet ones). These two conditions are not compatible if the basis functions are expressed in the deformed configuration as the locations of the boundaries will vary with the level of deformations or implicitly with time. However, these conditions are compatible if one proceeds in the undeformed configuration and thus $\mathbf{X}$ in Eq. (1), will denote the coordinates of a point in the undeformed configuration.

Accordingly, the equations of motion of an infinitesimal element can be expressed as (e.g. see [17,18], summation over repeated indices assumed)

$$\frac{\partial}{\partial X_k}\left(F_{ij}\, S_{jk}\right)+\rho_0\, b_i^0=\rho_0\, \ddot{u}_i \quad \text{for } \mathbf{X}\in \Omega_0 \tag{2}$$

where $\mathbf{S}$ denotes the second Piola–Kirchhoff stress tensor, ρ_0 is the density in the reference configuration, and $\mathbf{b}^0$ is the vector of body forces, all of which are assumed to depend on the coordinates X_i. Further, in Eq. (2), the deformation gradient tensor $\mathbf{F}$ is defined by its components F_{ij} as

$$F_{ij}=\frac{\partial x_i}{\partial X_j}=\delta_{ij}+\frac{\partial u_i}{\partial X_j}, \tag{3}$$

where δ_{ij} denotes the Kronecker delta and the displacement vector is $\mathbf{u}=\mathbf{x}-\mathbf{X}$, $\mathbf{x}$ being the position vector in the deformed configuration. Finally, Ω_0 denotes the domain occupied by the structure which has a boundary $\partial\Omega_0$ composed of two parts: $\partial\Omega_0^t$ on which the tractions $\mathbf{t}^0$ are given and $\partial\Omega_0^u$ on which the displacements are specified (assumed zero here). Thus, the boundary conditions associated to Eq. (2) are

$$F_{ij}\, S_{jk}\, n_k^0=t_i^0 \text{ for } \mathbf{X}\in \partial\Omega_0^t, \tag{4}$$

and

$$\mathbf{u}=\mathbf{0} \quad \text{for } \mathbf{X}\in \partial\Omega_0^u. \tag{5}$$

Note in Eqs. (2) and (4) that the vectors $\mathbf{b}^0$ and $\mathbf{t}^0$ correspond to the transport ("pull back") of the body forces and tractions applied on the deformed configuration, i.e. $\mathbf{b}$ and $\mathbf{t}$, back to the reference configuration (see [17,18]).

To complete the formulation of the elastodynamic problem, it remains to specify the constitutive behavior of the material. In this regard, it will be assumed here that the second Piola–Kirchhoff stress tensors $\mathbf{S}$ is linearly related to the Green strain tensor $\mathbf{E}$ defined as

$$E_{ij}=\frac{1}{2}\left(F_{ki}F_{kj}-\delta_{ij}\right) \tag{6}$$

That is,

$$S_{ij}=C_{ijkl}\, E_{kl}, \tag{7}$$

where C_{ijkl} denotes the fourth order elasticity tensor.

Introducing the assumed displacement field of Eq. (1) in Eqs. (2)–(7) and proceeding with a Galerkin approach leads, after some manipulations (see [19] for discussion and some symmetry and positive definiteness properties), to the desired

governing equations, i.e.

$$M_{ij}\ddot{q}_j + D_{ij}\dot{q}_j + K^{(1)}_{ij}\, q_j + K^{(2)}_{ijl} q_j q_l + K^{(3)}_{ijlp} q_j q_l q_p = F_i \tag{8}$$

in which the damping term $D_{ij}\,\dot{q}_j$ has been added to model the dissipation mechanisms on the structure.

Once the generalized coordinates $q_j(t)$ have been determined from Eq. (8), the stress field can also be evaluated from Eqs. (3), (6), and (7). Specifically, it is found that every component of the second Piola–Kirchhoff stress tensor can be expressed as

$$S_{ij} = \overline{S}_{ij} + \sum_{m=1}^{M} \hat{S}^{(m)}_{ij} q_m + \sum_{m,n=1}^{M} \tilde{S}^{(m,n)}_{ij} q_m\, q_n \tag{9}$$

where the coefficients $\overline{S}_{ij}$, $\hat{S}^{(m)}_{ij}$, and $\tilde{S}^{(m,n)}_{ij}$ depend only on the point $\mathbf{X}$ considered (see Section 4 for the identification of these coefficients). An alternate approach for the evaluation of the stresses has also been utilized [20] in which the elements of interest are subjected to the displacement field predicted by Eq. (1) within the finite element software and the resulting stresses produced.

3.2. Static condensation approximation

The governing equations for the full finite element model can be derived as in Eqs. (1)–(8) but with the coordinates q_i replaced by the finite element degrees of freedom y_i and the basis functions $\psi^{(n)}_i(\mathbf{X})$ becoming the element interpolation functions. This process accordingly leads to the equations

$$\hat{M}_{ij}\,\ddot{y}_j + \hat{D}_{ij}\,\dot{y}_j + \hat{K}^{(1)}_{ij}\, y_j + \hat{K}^{(2)}_{ijl}\, y_j y_l + \hat{K}^{(3)}_{ijlp}\, y_j y_l y_p = f_i \tag{10}$$

Introducing in Eq. (10) a modal expansion of the form of Eq. (1), i.e.

$$\mathbf{y}(t) = \sum_{n=1}^{M} q_n(t)\, \boldsymbol{\varphi}^{(n)} \tag{11}$$

where $\boldsymbol{\varphi}^{(n)}$ are basis functions and $q_n(t)$ are the associated generalized coordinates recovers Eq. (8) as expected.

Note that Eq. (10) was obtained without any approximation to the strain definition of Eq. (6). Yet, simplifications of it by the removal of selected nonlinear terms, more specifically the use of the von Karman strain definition [17], are often employed. To reflect the implications of this assumption, it is convenient to partition the degrees of freedom y_i into transverse (bending) $y_{b,i}$ and in-plane (membrane) $y_{m,i}$ components.

Then, neglecting damping, it is found that

$$\hat{M}_{b,ij}\,\ddot{y}_{b,j} + \hat{K}^{(1)}_{b,ij}\, y_{b,j} + \hat{K}^{(1)}_{bm,ij}\, y_{m,j} + \hat{K}^{(2)}_{b,ijl}\, y_{b,j}\, y_{b,l} + \hat{K}^{(3)}_{b,ijlp}\, y_{b,j}\, y_{b,l}\, y_{b,p} = f_{b,i} \tag{12}$$

$$\hat{M}_{m,ij}\,\ddot{y}_{m,j} + \hat{K}^{(1)}_{mb,ij}\, y_{b,j} + \hat{K}^{(1)}_{m,ij}\, y_{m,j} + \hat{K}^{(2)}_{mb,ijl}\, y_{b,j}\, y_{b,l} = f_{m,i} \tag{13}$$

where the *bm* and *mb* subscripts are used for the bending–membrane coupling terms. Note in these equations that the bending Eq. (12) is similar to its full counterpart of Eq. (10) with the membrane degrees of freedom involved linearly. Notable simplifications of the in-plane equations have occurred with the presence of only linear terms of the membrane degrees of freedom and quadratic of the bending ones.

These properties facilitate the static condensation of the in-plane degrees of freedom into the transverse ones [21–23] by neglecting the inertia associated with the in-plane motion, i.e.,

$$\hat{M}_{m,ij}\,\ddot{y}_{m,j} = 0 \tag{14}$$

In doing so, the membrane displacements can be expressed in terms of the bending displacements from Eq. (13) as

$$y_{m,p} = -[\hat{K}^{(1)}_{m}]^{-1}_{pi}[\hat{K}^{(1)}_{mb,ij}\, y_{b,j} + \hat{K}^{(2)}_{mb,ijl}\, y_{b,j}\, y_{b,l} - f_{m,i}] \tag{15}$$

Substituting Eq. (15) into Eq. (12) results in an equation of motion with the in-plane degrees of freedom statically condensed onto the transverse ones. The resulting equation is lengthy and its explicit form can be found in [23]. Note that this substitution involves obtaining products of several matrices and tensors characterizing the nonlinearity. Thus, the static condensation process effectively alters the form of the linear, quadratic and cubic stiffness terms when compared with the transverse degrees of freedom-related components of the stiffness terms of Eq. (12).

Nevertheless, the form of the equations of motion remains the same as Eq. (10). Specifically, performing the above stated manipulations and introducing a linear damping term leads to the equation of motion for the transverse degrees of freedom as

$$\hat{M}_{b,ij}\,\ddot{y}_{b,j} + \tilde{D}_{b,ij}\,\dot{y}_{b,j} + \tilde{K}^{(1)}_{b,ij}\, y_{b,j} + \tilde{K}^{(2)}_{b,ijl}\, y_{b,j}\, y_{b,l} + \tilde{K}^{(3)}_{b,ijlp}\, y_{b,j}\, y_{b,l}\, y_{b,p} = \tilde{f}_{b,i} \tag{16}$$

with tensors $\tilde{K}^{(1)}_{b,ij}$, $\tilde{K}^{(2)}_{b,ijl}$, and $\tilde{K}^{(3)}_{b,ijlp}$ different from $\hat{K}^{(1)}_{b,ij}$, $\hat{K}^{(2)}_{b,ijl}$, and $\hat{K}^{(3)}_{b,ijlp}$ of Eq. (12).

Applying to Eq. (16) the modal transformation

$$\mathbf{y}_b(t) = \sum_{n=1}^{L} q_{b,n}(t)\boldsymbol{\varphi}_b^{(n)} \tag{17}$$

where $\boldsymbol{\varphi}_b^{(n)}$ are basis functions representing the transverse displacements only and $q_{b,n}(t)$ are the corresponding generalized coordinates, leads to reduced order equations of the form

$$\overline{M}_{ij}\ddot{q}_{b,j} + \overline{D}_{ij}\dot{q}_{b,j} + \overline{K}_{ij}^{(1)} q_{b,j} + \overline{K}_{ijl}^{(2)} q_{b,j}\, q_{b,l} + \overline{K}_{ijlp}^{(3)} q_{b,j}\, q_{b,l}\, q_{b,p} = \overline{f}_i \tag{18}$$

where the modal masses $\overline{M}_{ij}$, damping terms $\overline{D}_{ij}$, stiffnesses $\overline{K}_{ij}^{(1)}$, $\overline{K}_{ijl}^{(2)}$ and $\overline{K}_{ijlp}^{(3)}$, and excitation $\overline{f}_i$ are dependent on the modal basis selected. Note that Eq. (18) is identical in form to Eq. (8). The key differences being that Eq. (18) governs the transverse displacement only, with the in-plane ones then expressed by Eq. (15), while the generalized coordinates of Eq. (8) affect all displacements.

Note that static condensation implies a memoryless map between the transverse and membrane displacements and thus the obtained in-plane response will exhibit the same frequency characteristics as the transverse one with additional combination frequencies induced by the nonlinearity of the map. Within its assumptions it is a successful approach and, for a transverse dominated problem, the effect of static condensation on the in-plane response was shown to be negligible [23].

4. Determination of ROM parameters

The next task in the formulation of a ROM is the determination of its stiffness coefficients from a structural model. In keeping with the focus of this review, the structural models considered here will be finite element based and one can envision 2 distinct approaches. The first one, referred to as "direct" here (see Section 4.1) is intrusive as it explicitly expresses the nonlinear stiffness coefficients within the finite element formulation. It is possible with open source codes in which the necessary information can be extracted. This approach is not the focus of the present review and thus Section 4.1 only highlights its major steps.

The second class of approaches, focused upon in this review, will be referred to as "indirect". They are non-intrusive and thus can be used with any commercial finite element package that has a static nonlinear solver such as Nastran and Abaqus. Two variations exist in this indirect class. In the first one (see Section 4.2), a series of static *displacement* fields are imposed and the forces required to achieve them determined from the finite element model. Imposing that the reduced order model match this data provides a simple set of equations from which the ROM parameters are recursively computed. In the second variation (see Section 4.3), a series of static *load* cases are imposed and the corresponding responses are determined. The parameters of the ROM are then obtained by a least squares solution of the resulting set of equations. The derivations presented in the ensuing sections are general with respect to the coefficients $K_{ij}^{(1)}$, $K_{ijl}^{(2)}$, and $K_{ijlp}^{(3)}$ although some of these can be shown to vanish in certain cases due to symmetry of the problem (e.g. flat isotropic structure) or due to a particular property of the finite element modeling. Further, some expected relations between coefficients (e.g. see [19,20]) have been derived and could be used in their identification. It should finally be noted that the experimental identification of the reduced order model stiffness coefficients has also been investigated, e.g. see [24].

4.1. Direct method

The direct method is based on the relationship between the finite element tensors and their modal counterparts, i.e. between $\hat{M}_{ij}$, $\hat{K}_{ij}^{(1)}$, $\hat{K}_{ijl}^{(2)}$, $\hat{K}_{ijlp}^{(3)}$, f_i and M_{ij}, $K_{ij}^{(1)}$, $K_{ijl}^{(2)}$, $K_{ijlp}^{(3)}$, and F_i for a formulation including all degrees of freedom (e.g. see [22]) or between $\hat{M}_{b,ij}$, $\tilde{K}_{b,ij}^{(1)}$, $\tilde{K}_{b,ijl}^{(2)}$, $\tilde{K}_{b,ijlp}^{(3)}$, $\tilde{f}_{b,i}$ and $\overline{M}_{ij}$, $\overline{K}_{ij}^{(1)}$, $\overline{K}_{ijl}^{(2)}$, $\overline{K}_{ijlp}^{(3)}$, $\overline{f}_i$ if static condensation is applied (e.g. see [23]). Specifically, proceeding with a full formulation and combining Eq. (11) into Eq. (10) and collecting terms leads to the relations

$$\begin{aligned} &M_{ij} = \varphi_p^{(i)}\hat{M}_{pr}\varphi_r^{(j)} \qquad F_i = \varphi_p^{(i)} f_p \qquad K_{ij}^{(1)} = \varphi_p^{(i)}\ \hat{K}_{pr}^{(1)}\varphi_r^{(j)} \\ &K_{ijl}^{(2)} = \hat{K}_{prs}^{(2)}\ \varphi_p^{(i)}\varphi_r^{(j)}\varphi_s^{(l)} \quad \text{and} \quad K_{ijlp}^{(3)} = \hat{K}_{rsuv}^{(2)}\ \varphi_r^{(i)}\varphi_s^{(j)}\varphi_u^{(l)}\ \varphi_v^{(p)} \end{aligned} \tag{19a)–(19e}$$

Then, given the availability of the matrices and tensors $\hat{M}_{ij}$, $\hat{K}_{ij}^{(1)}$, $\hat{K}_{ijl}^{(2)}$, $\hat{K}_{ijlp}^{(3)}$, f_i, a direct computation of the reduced order model parameters M_{ij}, $K_{ij}^{(1)}$, $K_{ijl}^{(2)}$, $K_{ijlp}^{(3)}$, and F_i proceeds from Eq. (19) for a particular choice of basis functions $\boldsymbol{\varphi}^{(n)}$ of components $\varphi_p^{(n)}$, see discussion in Sections 5 and 7 for application specific bases.

The key challenge of this direct approach is that the tensors $\hat{K}_{ijl}^{(2)}$ and $\hat{K}_{ijlp}^{(3)}$ are not available from most commercial finite element software, and in fact are generally not computed as such. This difficulty is then resolved by proceeding with an indirect identification of the reduced order model parameters as described in the ensuing sections.

4.2. Displacement-based indirect method

The use of indirect methods is necessary when the finite element tensors of quadratic and cubic stiffness terms, e.g. $\hat{K}^{(2)}_{ijl}$ and $\hat{K}^{(3)}_{ijlp}$, are not available. In such cases, the modal mass and forces, M_{ij} and F_i, are still determined from Eq. (19) but the determination of the reduced order model stiffness coefficients, $K^{(1)}_{ij}$, $K^{(2)}_{ijl}$, and $K^{(3)}_{ijlp}$, must be accomplished directly from Eq. (8) as an *evaluation* process.

One such process relies on the imposition on the finite element model of specified displacement fields of the form of Eq. (11). Then, the ith component of the nonlinear modal restoring force vector is expressed as

$$F^r_{\mathrm{NL},i} = K^{(1)}_{ij} q_j + K^{(2)}_{ijl} q_j q_l + K^{(3)}_{ijlp} q_j q_l q, \quad i = 1,\ldots,M, \tag{20}$$

Using a nonlinear static finite element analysis, the nonlinear restoring forces f^r_{NL} corresponding to each prescribed displacement field are computed in physical degrees of freedom and transformed to generalized coordinates per Eq. (19b), i.e.

$$F^r_{\mathrm{NL},i} = \varphi^{(i)}_p f^r_{\mathrm{NL},p} \tag{21}$$

As the forces $F^r_{\mathrm{NL},i}$ and the generalized coordinates q_i are known, Eq. (20) then constitutes a system of algebraic equations from which the linear, quadratic, and cubic reduced order model stiffness coefficients may be determined.

The procedure is demonstrated here for coefficients having all the same lower indices, that is, for $K^{(1)}_{ij}$, $K^{(2)}_{ijj}$, and $K^{(3)}_{ijjj}$, $i=1,\ldots, M$. For example, for $j=1$, a set of three displacement fields are prescribed [25,26]:

$$\mathbf{y} = q_1\ \boldsymbol{\varphi}^{(1)} \qquad \mathbf{y} = -q_1\ \boldsymbol{\varphi}^{(1)} \qquad \mathbf{y} = \hat{q}_1\ \boldsymbol{\varphi}^{(1)} \tag{22}$$

The modal displacements q_1 and $\hat{q}_1$ are two different scalar quantities and are specified such that the magnitude of the prescribed physical displacement field $\boldsymbol{y}$ is physically meaningful. The corresponding nonlinear restoring force is evaluated using the nonlinear static solution within a commercial finite element program, and is given as

$$\begin{aligned} F^{r1}_{\mathrm{NL},i} &= K^{(1)}_{i1} q_1 + K^{(2)}_{i11} q_1^2 + K^{(3)}_{i111} q_1^3 \\ F^{r2}_{\mathrm{NL},i} &= -K^{(1)}_{i1} q_1 + K^{(2)}_{i11} q_1^2 - K^{(3)}_{i111} q_1^3 \\ F^{r3}_{\mathrm{NL},i} &= K^{(1)}_{i1} \hat{q}_1 + K^{(2)}_{i11} \hat{q}_1^2 + K^{(3)}_{i111} \hat{q}_1^3 \end{aligned} \tag{23}$$

from which the coefficients $K^{(1)}_{i1}$, $K^{(2)}_{i11}$, and $K^{(3)}_{i111}$ are obtained. The remaining coefficients $K^{(1)}_{ij}$, $K^{(2)}_{ijj}$, and $K^{(3)}_{ijjj}$, $j=2,\ldots,M$, are determined in an analogous manner. It has been observed in [25] that the stiffness coefficients obtained via this approach are not sensitive to the particular value of modal displacement specified.

A similar technique can be employed to determine stiffness coefficients with two unequal lower indices, e.g. $K^{(2)}_{i12}$, $K^{(3)}_{i112}$, and $K^{(3)}_{i122}$. Coefficients of this type appear only if the number of retained eigenvectors is greater than or equal to two ($M \geq 2$). Prescribing the displacement fields

$$\mathbf{y} = q_1\ \boldsymbol{\varphi}^{(1)} + q_2\ \boldsymbol{\varphi}^{(2)} \qquad \mathbf{y} = -q_1\ \boldsymbol{\varphi}^{(1)} - q_2\ \boldsymbol{\varphi}^{(2)} \qquad \mathbf{y} = q_1\ \boldsymbol{\varphi}^{(1)} - q_2\ \boldsymbol{\varphi}^{(2)} \tag{24}$$

allows the coefficients $K^{(2)}_{i12}$, $K^{(3)}_{i112}$, and $K^{(3)}_{i122}$ to be determined. All remaining coefficients of the type $K^{(2)}_{ijl}$, $K^{(3)}_{ijjl}$, and $K^{(3)}_{ijll}$ for $l > j = 1, 2,\ldots, M$ are found in this manner. Finally, for cases when the number of retained eigenvectors is greater than or equal to three ($M \geq 3$), coefficients with three unequal lower indices, e.g. $K^{(3)}_{i123}$, are determined by prescribing the displacement field

$$\mathbf{y} = q_1\ \boldsymbol{\varphi}^{(1)} + q_2\ \boldsymbol{\varphi}^{(2)} + q_3\ \boldsymbol{\varphi}^{(3)} \tag{25}$$

All remaining coefficients of type $K^{(3)}_{ijlp}$, $p > l > j = 1, 2,\ldots, M$ are found in this manner.

The number of unknown coefficients, and hence the number of nonlinear static solutions required for a transformation utilizing M modes is

$$\text{Number of NL static solutions} = 3\binom{M}{1} + 3\binom{M}{2} + \binom{M}{3}, \quad M \geq 3 \tag{26}$$

where

$$\binom{M}{k} = \frac{M!}{k!\ (M-k)!} \tag{27}$$

Note that the three terms in Eq. (26) reflect the number of linear, quadratic, and cubic modal stiffness coefficients, respectively. The number of nonlinear static solutions can be viewed as a measure of the fixed cost of the reduced order analysis, as the modal reduction must be performed regardless of the simulated response time to be eventually computed. A modification of the above algorithm which utilizes the tangent stiffness matrix of the full finite element model and matches it to the one of the reduced order model has recently been proposed and demonstrated [27]. It does lead to a

notable reduction in computational cost but is applicable only to those commercial finite element codes that allow the output of the tangent stiffness matrix.

The procedure described above is readily extended to the identification of the coefficients $\overline{S}_{ij}$, $\hat{S}_{ij}^{(m)}$, and $\tilde{S}_{ij}^{(m,n)}$ of the stress representation, Eq. (9), provided that the desired stresses are computed (the components and locations of interest only) in the application of the displacement fields of Eqs. (22) and (24) [26].

4.3. Force-based indirect method

Another way to evaluate the coefficients in the nonlinear reduced order model is through regression analysis using a set of prescribed static loads applied to the finite element model $\mathbf{f}^{(s)}$[28,29]. These loads are selected in the form

$$\mathbf{f}^{(s)} = a_r^{(s)}\ \boldsymbol{\varphi}_r^{(s)} \tag{28}$$

i.e. as scaled, linear combinations of the basis functions (which were selected as described in Section 5). For each load case s, the displacement vector $\mathbf{y}^{(s)}$ of all degrees of freedom of the finite element model is obtained and projected on the basis functions $\boldsymbol{\varphi}^{(n)}$ of Eq. (11) to yield the corresponding generalized coordinates $q_i^{(s)}$. Inserting these values in Eq. (8) leads to the relations

$$K_{ij}^{(1)}\ q_j^{(s)} + K_{ijl}^{(2)} q_j^{(s)} q_l^{(s)} + K_{ijlp}^{(3)}\ q_j^{(s)} q_l^{(s)} q_p^{(s)} = \varphi_j^{(i)}\ f_j^{(s)} \tag{29}$$

which can be used for the identification of the coefficients $K_{ij}^{(1)}$, $K_{ijl}^{(2)}$, $K_{ijlp}^{(3)}$. With sufficient loading cases, a system of equations is developed, and these coefficients are then identified mode-by-mode, i.e. for each value of i independently, in a least-squares sense. The linear stiffness coefficients $K_{ij}^{(1)}$ can either be identified along with the nonlinear one, or, having already been calculated from Eq. (19c), used as a further constraint to the identification problem.

The vectors $\mathbf{f}^{(s)}$ are selected to exercise the desired nonlinear effects and identify the linear and nonlinear coefficients [30]. To select the load cases for the regression analysis, a nodal point of interest on the structure is identified, along with a linear estimate of the desired displacement for that location. Different load scale factors $a_r^{(s)}$ to be used in Eq. (28) are then selected based on desired transverse displacements that range from a small fraction of the panel thickness to displacements equal to or more than the panel thickness. This ensures that the desired nonlinear effects are well represented in the coefficient identification procedure. The desired displacement at the points of interest naturally leads to a scaling of the basis functions that make up the load vectors. For example, the rth load scale factor, $a_r^{(s)}$, based on a linear estimate of displacements, can be obtained for the modal basis of Section 5.1as

$$a_r^{(s)} = \frac{\omega_r^2}{\boldsymbol{\varphi}^{(r)T}\boldsymbol{\varphi}^{(r)}}\ \frac{W_c}{\varphi_c^{(r)}} \tag{30}$$

where ω_r is the natural frequency of the mode $\boldsymbol{\varphi}^{(r)}$, W_c the desired transverse displacement at location "c", and $\varphi_c^{(r)}$ the transverse displacement of $\boldsymbol{\varphi}^{(r)}$ at location "c" [31]. A post-processing check of the ratio of linear-to-nonlinear displacement at location "c" gives an indication of the degree of nonlinearity resulting from the applied load cases.

5. Modal bases

As stated in the introduction, one of the key aspects of the reduced order modeling effort is the selection of the basis functions $\boldsymbol{\varphi}^{(r)}$. If the structural response is not well represented within this basis, the corresponding prediction of the reduced order model will in general be poor. In linear dynamic problems, the construction of the basis is usually quite straightforward and consists in selecting the linear modes $\hat{\boldsymbol{\varphi}}_r$ of the lightly damped structure, defined as

$$\hat{\mathbf{K}}^{(1)}\hat{\boldsymbol{\varphi}}_r = \omega_r^2\ \hat{\mathbf{M}}\ \hat{\boldsymbol{\varphi}}_r, \tag{31}$$

of natural frequency ω_r in the band of the excitation, e.g. [32], assumed here to be generally well separated (i.e. in the "low frequency" band, see [33]). Because the problems of interest tend to be dominated by the transverse motion, low frequency transverse-dominated modes typically comprise the basis when linearity can be assumed. However, as the amplitude of the response increases, geometrically nonlinear effects arise which include (i) a change of stiffness of the transverse motions which is globally hardening through its cubic terms but may (e.g. for a curved panel) also exhibit a local softening induced by the quadratic terms. Also included is (ii) a significant increase in in-plane motions induced by the nonlinear coupling of the transverse and in-plane displacements. Through this coupling mechanism, the in-plane motions also affect the transverse ones and this effect is typically a significant softening referred to as the "membrane stretching" effect. These observations have led to two separate approaches for the basis selection.

The first approach (the "condensed basis", see Section 5.1) relies on retaining only linear transverse modes, as in the linear case with the possible addition of a few out of band modes, and treating the in-plane displacements as unobserved variables, typically eliminating them (implicitly) through a static condensation (see Section 3.2) which accounts for the membrane stretching effect. In the second approach (the "full bases", see Sections 5.2–5.4), the modeling of all displacements is performed with a basis that includes the linear modes directly excited additionally enriched to complete the representation of the in-plane displacements. Within the focus of the present review, this enrichment has been achieved with either linear modes residing above or well above the excitation bandwidth (Section 5.2) or "dual" modes

obtained from nonlinear static solutions (Section 5.3). System identification methods are also described (Section 5.4) to guide the selection of the linear modes to be selected in Section 5.2.

Each of these basis selection strategies has been successfully validated and can be used with either the force or displacement based parameter identification methods of Sections 4.2 and 4.3, although some natural pairings between basis choice and identification method occur. Each basis selection strategy has its own advantages/merits in terms of number of basis functions used, accuracy in representing the response, and complexity in obtaining the basis.

5.1. Condensed/transverse modes only basis

For aircraft structures under transverse loading, the in-plane response is closely quasi-static and softens or reduces the stiffness of the model in large displacement response [34] through membrane stretching. This observation suggests the applicability of some of the static condensation concepts of Section 3.2 and has led to the consideration of only transverse, bending modes while *implicitly retaining the effect of membrane softening*. This approach was originally proposed in [28,29] and is related to the experimental identification efforts of [24]. The need to capture the membrane softening effects when only bending modes are considered in the basis has been established clearly in [30].

The basis considered in this section, see [35,36], is composed of 2 sets of functions, $\boldsymbol{\varphi}_b^{(r)}$ and $\boldsymbol{\varphi}_m^{(r)}$, that focus on characterizing the bending and membrane dominated motions. The former set comprises the linear modes of the *full* finite element model, Eq. (10), not of the condensed one, Eq. (16), i.e. $\boldsymbol{\varphi}_b^{(r)} = \hat{\boldsymbol{\varphi}}_u$ for $r=1,\ldots,M$, and values of u such that the linear mode $\hat{\boldsymbol{\varphi}}_u$ is bending dominated. Note that these modes contain in general, e.g. for a curved structure, small membrane contributions which capture some, but not all of the in-plane stretching effects directly. This observation has led to the introduction of a second part of the basis, referred to collectively as the membrane modes $\boldsymbol{\varphi}_m^{(r)}$ [35,36] so that the finite element response $\mathbf{y}$ is modeled as

$$\mathbf{y}(t) = \mathbf{y}_b(t) + \mathbf{y}_m(t) = \sum_{n=1}^{M} q_{b,n}(t)\boldsymbol{\varphi}_b^{(n)} + \sum_{n=1}^{M'} q_{m,n}(t)\,\boldsymbol{\varphi}_m^{(n)} \tag{32}$$

The retained bending-dominated modes $\boldsymbol{\varphi}_b^{(n)}$ are typically those that are directly excited by the loading, i.e., those modes within the excitation band plus additional ones depending on the application and anticipated response. For instance, curved structures can exhibit antisymmetric behavior near a snap-through bifurcation even if the loading is purely symmetric, and thus antisymmetric mode shapes would need to be included in the basis. Another example would be those cases of excessive deformation such as panel snap-through (on the order of many panel thicknesses), where additional modes must be included to accurately predict the post-buckled displacement and stress response [36].

In keeping with the static condensation perspective, the bending related generalized coordinates $q_{b,n}(t)$ will be governed by Eq. (8) while the membrane component of the response $\mathbf{y}_m(t)$ will be obtained from the bending part $\mathbf{y}_b(t)$ in a manner similar to Eq. (15) but without the linear terms which have been included in the eigenvalue problem of Eq. (31) (see [35]). That is, $\mathbf{y}_m(t)$ should be a pure quadratic form of the coordinates $q_{b,n}(t)$. This property can be reflected in Eq. (32) by selecting $M' = M(M+1)/2$ and

$$\begin{aligned}[q_{m,1}(t)\; q_{m,2}(t)\cdots q_{m,M'}(t)] = [q_{b,1}^2(t) \quad & q_{b,1}(t)\,q_{b,2}(t) \quad q_{b,1}(t)\,q_{b,3}(t) \;\cdots\; q_{b,1}(t)\,q_{b,M}(t) \\ & q_{b,2}^2(t) \quad q_{b,2}(t)\,q_{b,3}(t) \;\cdots q_{b,2}(t)\,q_{b,M}(t) \;\cdots\; q_{b,M}^2(t)\Big]\end{aligned} \tag{33}$$

It remains then to define the corresponding membrane basis functions $\boldsymbol{\varphi}_m^{(n)}$. It was proposed in [35] to identify them from a given set of observed responses $\mathbf{y}^{(s)}$, $s=1, 2,\ldots,S$, e.g. obtained during the identification of the coefficients of the equations governing the bending coordinates $q_{b,n}(t)$. After estimating the corresponding bending components $\mathbf{y}_b^{(s)}$ and the generalized coordinates $q_{b,n}^{(s)}$, the membrane components of the response $\mathbf{y}_m^{(s)}$ and their associated generalized coordinates $q_{m,n}^{(s)}$ are obtained from Eq. (32), i.e. $\mathbf{y}_m^{(s)} = \mathbf{y}^{(s)} - \mathbf{y}_b^{(s)}$, and Eq. (33). Then, the membrane basis functions can be estimated as [35]

$$[\boldsymbol{\varphi}_m^{(1)}\boldsymbol{\varphi}_m^{(2)}\ldots\boldsymbol{\varphi}_m^{(M)}] = \mathbf{Y}_m\mathbf{Q}^T\left(\mathbf{Q}\,\mathbf{Q}^T\right)^{-1} \tag{34}$$

where

$$\mathbf{Y}_m = \left[\mathbf{y}_m^{(1)}\mathbf{y}_m^{(2)},\ldots,\mathbf{y}_m^{(S)}\right] \quad \text{and} \quad Q_{ij} = q_{m,i}^{(j)} \tag{35}$$

The method described above has been termed the Implicit Condensation with Expansion (ICE) approach, where expansion refers to the inclusion of the identified membrane basis. This approach represents an extension of the Implicit Condensation (IC) method [30] in which no membrane component y_m is explicitly present but the membrane softening is still implicitly included in the model. Note that both the IC and ICE approach assume a statically condensed form of the structural model for identification of the bending generalized coordinate coefficients as shown in Eq. (29). The ICE approach extends the IC one by using the bending generalized coordinates to identify a membrane basis and the associated softening effect explicitly. More specifically, this effect is/must be reflected in the linear, quadratic, and cubic coefficients of Eq. (8) governing the bending generalized coordinates $q_{b,n}^{(s)}$. In fact, large differences, e.g. 50%, in nonlinear stiffness

coefficients do result if the membrane softening is not included in the identification process (see [30] for discussion and [14] for a related comparison), as expected.

This requirement affects how the identification techniques of Section 4 are applied. The force-based indirect method, Section 4.3, is most natural to apply as it is then only necessary that the loads imposed on the structure promote the bending deformations. Nevertheless, the application of the displacement-based approach of Section 4.2 is also possible and has been demonstrated in flat structures [14]. In this case, the transverse displacements were imposed while those in the in-plane direction were left unconstrained and thus were effectively statically condensed. This procedure led to a very well identified model (see [14]).

Note finally that the stress response is ultimately the focus in acoustic fatigue prediction. In this regard, the IC approach does not accurately calculate the strain as it does not allow for the calculation of the membrane displacement. McEwan et al. [29] nevertheless proposed and demonstrated an additional estimation procedure between bending displacements and strains, involving a quadratic relation as Eq. (9), to arrive at the desired stress response. No such issue is encountered with the ICE approach which recovers the full displacement field.

5.2. Linear modes basis

The use of bases consisting solely of linear normal modes has been studied extensively and found to be applicable over a broad range of applications owing in particular to their property of being complete. It is important to recognize in the following that there are two types of couplings between transverse and in-plane displacements that may be present. A linear coupling is a property of the structural geometry and is independent of the magnitude of the response, e.g. a planar isotropic beam is linearly uncoupled while a curved arch is linearly coupled. The subsequent discussion applies to both types of linear coupling. The second mechanism is the nonlinear coupling due to the large deflection response. For such problems, a sufficient basis consists of modes which represent both the transverse and in-plane responses [19,20] while accurately capturing the nonlinear coupling between both responses.

Because of the computational effort associated with the nonlinear stiffness evaluation, Eqs. (26)–(27), and modal reduction there is an incentive to form a reduced order system capable of supporting multiple loading conditions. This implies that, for a given loading condition, the participation of certain modes used to form the reduced order system may be minimal. It was demonstrated that the inclusion of linear normal modes beyond those minimally required had no detrimental effect on the computed response [20,37–39]. Therefore, a so-called cumulative basis can be formed from the summation of bases identified from different loading conditions, as long as the modes used collectively are linearly independent. This implies that such a basis can be constructed when the modes are produced from the same eigen-analysis, that is, from the single stress-free or pre-stressed condition. The loading conditions themselves may differ in their magnitudes and/or their spatial distributions (Section 6). The simplest example of a modal basis applicable over a range of amplitudes is that of a single basis formed for the analysis of a nonlinear response, but applied to the analysis of the linear response.

Finally, the identification of participating linear modes is difficult in all but the simplest cases. Therefore, identification methods, such as the proper orthogonal decomposition (POD) discussed in Section 5.4, are generally needed to guide the basis selection in most cases.

5.3. Linear modes and dual modes basis

Other basis selection strategies have also been proposed that rely either only partially or not at all on the linear modes of the structure. This latter class of approaches includes in particular the proper orthogonal decomposition (POD) method, see [16,40] for some static applications with indirect evaluation of the stiffness coefficients. In the former group of strategies, the linear modes involved in the linear response determination are *enriched* by other basis functions suitably chosen, e.g. see [26,36,41,42] and references therein.

One such approach [26,36] to construct a full basis appropriate for the modeling of the nonlinear response is to focus specifically on capturing the membrane stretching effects in the enrichment. The key idea in this approach is thus to subject the structure to a series of "representative" static loadings, determine the corresponding *nonlinear* displacement fields, and extract from them additional basis functions, referred to as the "dual modes" that will be appended to the linear basis, i.e. the modes that would be used in the linear case. The arguments carried out below are presented in the context of a flat structure with membrane stretching in the in-plane direction and the linear displacements in the transverse one but the formulation is generic and has been demonstrated on a curved panel [36].

In this regard, note that the membrane stretching effect is induced by the nonlinear interaction of the transverse and in-plane displacements, not by an external loading. Thus, the dual modes can be viewed as associated (the adjective "companion" would have been a better description than "dual") with the transverse displacements described by the linear basis. The representative static loadings should then be selected to excite primarily the linear basis modes and, in fact, in the absence of geometric nonlinearity (i.e. for a linear analysis) should only excite these modes, i.e. the applied load vectors $\mathbf{f}^{(m)}$ on the structural finite element model should be such that the corresponding linear static responses are of the

form

$$\mathbf{u}^{(m)} = \sum_i \alpha_i^{(m)}\, \boldsymbol{\varphi}^{(i)} \tag{36}$$

which occurs when

$$\mathbf{f}^{(m)} = \sum_i \alpha_i^{(m)}\, \hat{\mathbf{K}}^{(1)}\, \boldsymbol{\varphi}^{(i)} \tag{37}$$

where $\alpha_i^{(m)}$ are coefficients to be chosen with m denoting the load case number. A detailed discussion of the linear combinations to be used is presented in [26] but, in all validations carried out, it has been sufficient to consider the cases

$$\mathbf{f}^{(m)} = \alpha_i^{(m)}\, \hat{\mathbf{K}}^{(1)}\, \boldsymbol{\varphi}^{(i)}\,, \quad i = \text{dominant mode} \tag{38}$$

and

$$\mathbf{f}^{(m)} = \frac{\alpha_i^{(m)}}{2}\left[\hat{\mathbf{K}}^{(1)}\, \boldsymbol{\varphi}^{(i)} + \hat{\mathbf{K}}^{(1)}\, \boldsymbol{\varphi}^{(j)}\right], \quad i = \text{dominant mode}, j \neq i \tag{39}$$

where a "dominant" mode is loosely defined as one expected to provide a large component of the panel response to the physical loading. The ensemble of loading cases considered is formed by selecting several values of $\alpha_i^{(m)}$ for each dominant mode in Eq. (38) and also for each mode $j \neq i$ in Eq. (39). Note further that both positive and negative values of $\alpha_i^{(m)}$ are suggested and that their magnitudes should be such that the corresponding displacement fields $\mathbf{u}_i^{(m)}$ and $\mathbf{u}_{ij}^{(m)}$ range from near linear cases to some exhibiting a strong nonlinearity.

The next step of the basis construction is the extraction of the nonlinearity effects in the obtained displacement fields which is achieved by removing from the displacements fields their projections on the linear basis, i.e. by forming the vectors

$$\mathbf{v}_i^{(m)} = \mathbf{u}_i^{(m)} - \sum_j [\boldsymbol{\varphi}^{(j)T} \hat{\mathbf{M}} \mathbf{u}_i^{(m)}]\, \boldsymbol{\varphi}^{(j)} \quad \text{and} \quad \mathbf{v}_{ij}^{(m)} = \mathbf{u}_{ij}^{(m)} - \sum_j [\boldsymbol{\varphi}^{(j)T} \hat{\mathbf{M}} \mathbf{u}_{ij}^{(m)}] \boldsymbol{\varphi}^{(j)} \tag{40}$$

when the finite element mass matrix $\hat{\mathbf{M}}$ serves for the orthonormalization of the basis functions $\boldsymbol{\varphi}^{(j)}$ (including the linear basis functions and any dual mode already selected).

A proper orthogonal decomposition of each set of "nonlinear responses" $\mathbf{v}_i^{(m)}$ and $\mathbf{v}_{ij}^{(m)}$ is then sequentially carried out to extract the dominant features of these responses which are then selected as dual modes. The POD eigenvectors $\boldsymbol{\varphi}_k$ selected as dual modes should not only be associated with a large eigenvalue but should also induce a large strain energy, as measured by $\boldsymbol{\varphi}_k^T \hat{\mathbf{K}}^{(1)} \boldsymbol{\varphi}_k$, since the membrane stretching that the dual modes are expected to model is a stiff deformation mode.

A recent investigation [16] has demonstrated that the dual modes defined as above are strongly related to POD eigenvectors of response snapshots.

5.4. System identification for basis selection

A system identification based approach establishes a rigorous means of selecting the modal basis. Three variations of the system identification procedure are next discussed. The first is based solely on a proper orthogonal decomposition (POD) analysis [43,44] of the displacement response. The other two utilize aspects of a smooth orthogonal decomposition (SOD) analysis [45]. Each procedure utilizes short-duration response data from numerical simulation in physical degrees of freedom, test results [24,46] or combination of both [46].

5.4.1. POD-based approach

In the POD-based approach, a displacement snapshot matrix $\mathbf{U}$ can be formed as an accumulation of n instantaneous displacement fields (snapshots). The snapshot matrix contains a selected set of N degrees of freedom resulting in a matrix of size $n \times N$. The sample rate and spatial resolution of the snapshot matrix must be sufficient to resolve the system's temporal and spatial characteristics of interest. The displacement correlation matrix $\mathbf{R_U}$ of size $N \times N$, is formed as

$$\mathbf{R_U} = \frac{1}{n}\mathbf{U}^T\mathbf{U} \tag{41}$$

An eigen-analysis of the displacement correlation matrix $\mathbf{R_U}$ is next performed, i.e.,

$$\mathbf{R_U}\, \mathbf{p} = \mathbf{p}\, \boldsymbol{\Lambda} \tag{42}$$

to obtain the $N \times N$ proper orthogonal mode (POM) matrix $\mathbf{P} = [\mathbf{p}_1\ \mathbf{p}_2, \ldots, \mathbf{p}_N]$ and the diagonal proper orthogonal value (POV) matrix, $\boldsymbol{\Lambda}$ of elements λ_j [43].

The contribution of each POM to the overall dynamic response is given by

$$\chi_j = \frac{\lambda_j}{\sum_{j=1}^{N} \lambda_j}, \quad j = 1,\ldots,N \tag{43}$$

where χ_j is the jth POM modal amplitude participation factor. The sum of all POM modal amplitude participation factors is unity. When the dominant M POMs are selected, their cumulative participation, υ, can be expressed as

$$\upsilon = \sum_{j=1}^{M} \chi_j, \quad 0 < \upsilon \leq 1 \tag{44}$$

The retention of only M selected POMs reduces the size of $\mathbf{P}$ to $N \times M$.

The above POD-based identification process was successfully demonstrated on 1-D and 2-D thin-walled structures [37,47–49]. Because the identification procedure utilizes only displacement response data, the modal basis selection criterion relied solely on POM amplitudes. However, different degree of freedom types (e.g. transverse or in-plane displacements) often times exhibit significantly different response magnitudes. Therefore, the selection process had to be performed independently for each degree of freedom type to avoid discriminating against important response components having small amplitudes. This procedure for selecting POMs is subsequently referred to as the *modal amplitude participation* (MAP) procedure.

5.4.2. POD–SOD based approaches

A modified identification approach [50] to mitigate the need to process individual degree of freedom types separately in the basis selection process additionally includes velocity response data and utilizes aspects of the smooth orthogonal decomposition (SOD) analysis [45]. Specifically, the velocity correlation matrix $\mathbf{R_V}$, of size $N \times N$, is formed from the full-field velocity snapshot matrix $\mathbf{V}$ as

$$\mathbf{R_V} = \frac{1}{n}\mathbf{V}^T\mathbf{V}. \tag{45}$$

It can be shown that estimates of the POM frequencies, i.e. eigenvalues of Eq. (45), can be obtained from the Rayleigh quotient-like relationship [45,51]

$$\boldsymbol{\gamma}_P = \boldsymbol{\omega}_P^2 = \mathbf{1}\frac{\mathbf{P}^{-1}\mathbf{R}_V\mathbf{P}^{-T}}{\mathbf{P}^{-1}\mathbf{R}_U\mathbf{P}^{-T}} \tag{46}$$

where $\mathbf{1}$ is the identity matrix used to extract the diagonal and vector $\boldsymbol{\gamma}_P = \boldsymbol{\omega}_P^2$ contains estimated POM frequencies. The identification approach which retains POMs within some specified frequency bandwidth based on Eq. (46) is subsequently referred to as the *estimated POM frequencies* (EPF) [52].

The estimated POM frequencies can also be used to obtain the modal energy corresponding to a particular POM. Feeny and Liang [44] showed that for lightly damped randomly excited systems and large but finite number of simulation time steps n, the POVs approximate the mean square values of the modal coordinates $q_j^{(i)}$ of POM j, i.e.,

$$\lambda_j = \frac{1}{n}\sum_{i=1}^{n} [q_j^{(i)}]^2. \tag{47}$$

Note that the number of simulation time steps is typically greater than the number of time steps used in the correlation matrices for system identification. Assume that a measure of the instantaneous modal kinetic energy associated with the jth POM can be represented as

$$e_j^{(i)} \cong \omega_j^2 [q_j^{(i)}]^2 \tag{48}$$

The mean modal kinetic energy over n simulation time steps becomes

$$\bar{e}_j = \frac{1}{n}\sum_{i=1}^{n} e_j^{(i)} \tag{49}$$

Substituting Eq. (48) into Eq. (49) yields

$$\bar{e}_j \cong \omega_j^2 \sum_{i=1}^{n} [q_j^{(i)}]^2 \tag{50}$$

Further substituting Eqs. (46) and (47) into Eq. (50) yields the mean modal kinetic energy in terms of the POVs and their estimated squared frequencies as

$$\bar{e}_j \cong \gamma_j \lambda_j \tag{51}$$

As in Eq. (43), the contribution of each POM to the overall dynamic response is given by

$$\chi_j = \frac{\overline{e}_j}{\sum_{j=1}^{N} \overline{e}_j}, \quad j = 1,\ldots,N \tag{52}$$

where χ_j is now the jth POM modal energy participation factor. The sum of all POM modal energy participation factors is unity. Similarly, the cumulative participation is given by Eq. (44), using the POM modal energy participation factor in place of the POM modal amplitude participation factor. Retention of only M selected POMs reduces the size of $\boldsymbol{P}$ to N x M. The process through which modal energy is used for selecting POMs is subsequently referred to as the *modal energy participation* (MEP) procedure. For both the MAP or MEP approaches, a set of POMs may be selected based on the modal participation factor, the cumulative participation, or some combination thereof. However, unlike the MAP approach which requires as many criteria as there are degree of freedom types used in the system identification, e.g. one cutoff value for the transverse displacement and one value for the in-plane displacement, the MEP approach requires only a single criterion for either Eq. (52) or (44). The MEP procedure was also successfully tested by comparing the reduced order analysis results with those obtained from full-order simulations in physical degrees of freedom [52]. A comparison of all basis selection procedures (MAP, EPF and MEP) is given in [52] for three different nonlinear systems using the displacement-based indirect method of Section 4.2.

5.4.3. Identification guided basis selection

Because of the potentially high computational effort involved in the indirect evaluation of the nonlinear stiffness, there is an advantage to performing this operation once using a robust, load-independent basis. A basis constructed directly from the POMs does not form such a robust basis because the POMs are load-dependent . Therefore, in all three identification approaches (MAP, EPF and MEP), an additional step relating load-independent linear modes to load-dependent POMs may be undertaken. Use of linear modes only allows for the formation of a load-independent modal basis with the potential for supporting multiple analysis cases having varying excitation and response characteristics.

The relationship between the M selected POMs and the set of linear modes can be established using the modal assurance criterion (MAC) [47,48], or by representing each selected POM as an expansion of linear modes [37,49]. The MAC is used to compare each selected POM with up to the full number of linear modes. Linear modes with MAC values in excess of some cut-off, e.g. MAC ≥ 0.5, are then used to form the M size basis. This approach, while simple, may not identify any linear modes corresponding to a particular POM if that POM is highly distorted. A more versatile approach is to represent each selected POM as a superposition of linear modes. The expansion coefficient matrix $\mathbf{C}_{\text{exp}}$ is obtained as

$$\mathbf{C}_{\text{exp}} = \hat{\boldsymbol{\Phi}}^T \mathbf{P} = [\hat{\boldsymbol{\varphi}}_1 \hat{\boldsymbol{\varphi}}_2 \cdots \hat{\boldsymbol{\varphi}}_M]^T \mathbf{P}. \tag{53}$$

Each column of $\mathbf{C}_{\text{exp}}$ corresponds to a particular POM and provides the coefficients required for linear mode superposition. Since the POMs are not normalized, each column of coefficients is individually normalized such that its maximum value is unity. In this manner, a single cut-off value can be specified for all POMs. The cut-off value selection is arbitrary, but previous experience proved that a value of 0.5 gives reasonable results [37,49]. This technique guarantees that at least one linear mode will be identified for each selected POM. The end result of the basis selection process is a set of M selected linear modes, $M \ll N$, suitable for use with any of the direct or indirect nonlinear modal reductions. For statically condensed formulations, either the full set of M selected linear modes (inclusive of both bending and in-plane modes) can be applied, or a subset containing only bending modes.

6. Validations

The discussion of Sections 3–5 has emphasized the rationale for the cubic nonlinearity of the ROM governing equations, for the identification of its parameters, and for the selection of the basis functions. Ultimately, however, only a comparison of reduced order model predictions with an accurate baseline response can yield an assessment of the accuracy of the former. Even then, such successful validations are difficult to generalize owing to the many different effects that can be induced by the geometric nonlinearity. Accordingly, a fairly large set of validations have been carried out and a few typical examples are summarized here.

In these validations and wherever possible, the reduced order model predictions were compared with full finite element computations, the two being performed as closely one-to-one as possible. That is, the finite element model used for the full order predictions was the same as the one used for the identification of the ROM parameters (including the damping properties), the loading was selected to be identically the same, and the displacements/stresses compared were obtained at the same physical locations and directions. Yet, differences are expected that arise most notably from the numerical algorithms used to compute the response. The finite element results were obtained using Nastran and Abaqus while the reduced order model results were obtained by research codes performing the numerical integration of the ROM equations, typically by Newmark-β algorithms.

A key strength of finite element based reduced order models, especially those extracted from commercial software (Nastran, Abaqus, etc.), is the capability to treat models which are complex from geometry and/or boundary conditions. The first validation example was accordingly selected as one exhibiting both mixed elements (beams and plates) as well as

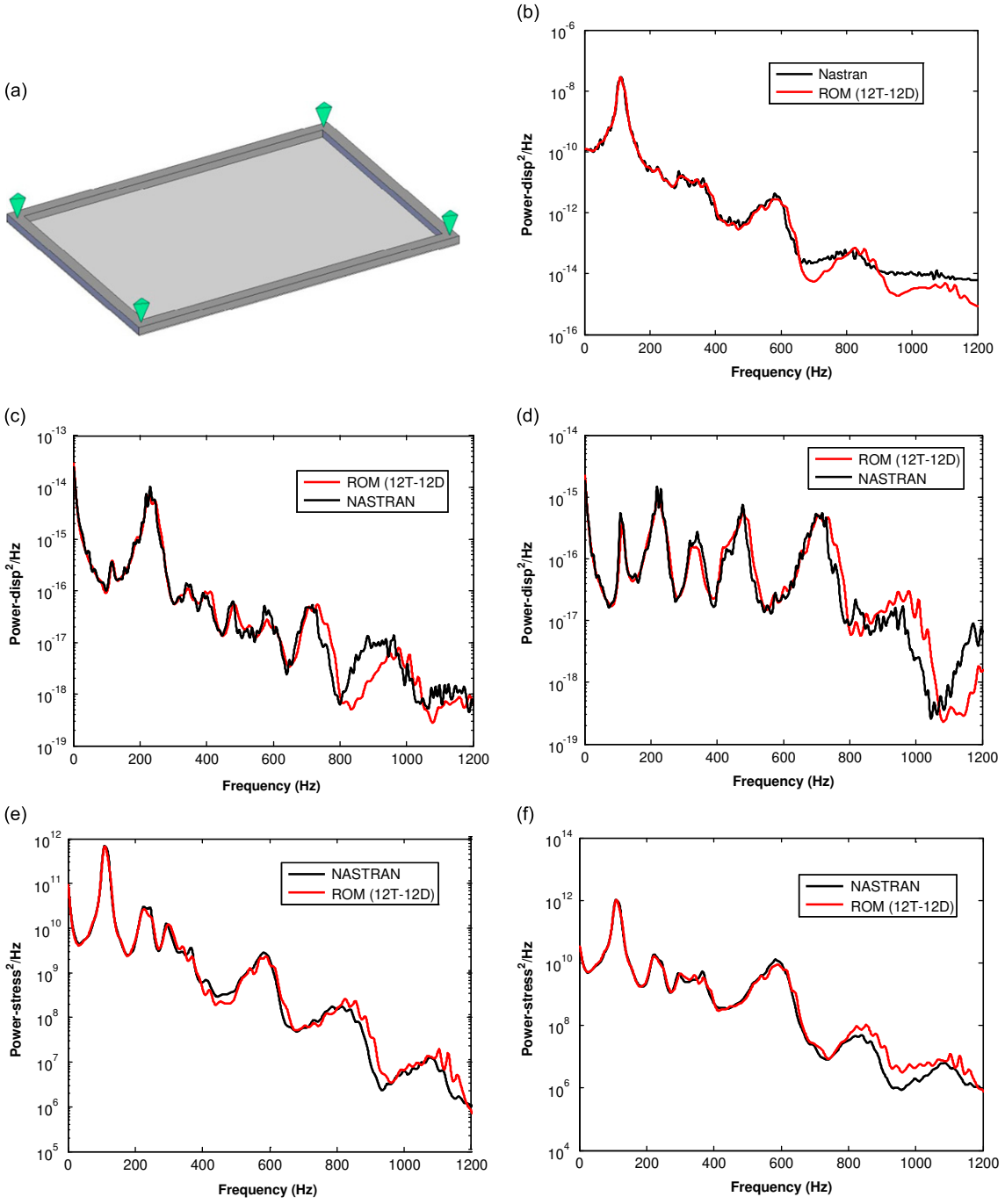

Fig. 1. Beam stiffened plate supported at its four corners: (a) model. Comparison of power spectra of (b) transverse displacement, (c) in-plane displacement (along long side), (d) in-plane displacement (along short side) and stresses (e) S_{xx} and (f) S_{yy} where x is along the long side of the panel and y along the short one.

non-standard boundary conditions (i.e. not fully clamped, simply supported, etc.). More specifically, an aluminum plate reinforced along its edges by an aluminum beam and supported at its four corners only was considered, see Fig. 1(a) and [26] for details. The panel was excited by a bandlimited white noise excitation in the band [0, 1048 Hz] equivalent to an acoustic excitation of overall sound pressure level of 147 dB. A 12 transverse—12 duals (based on mode 1 dominant, see Section 5.3) reduced order model was constructed using the displacement-based indirect method of Section 4.2. Shown in Fig. 1(b)–(g) are comparisons of displacements and stresses at a rather arbitrary point of the plate (node 55, see [26] for discussion and further comparisons) predicted by this ROM and Nastran. Note the clear qualitative and quantitative agreement of the reduced order and finite element predictions.

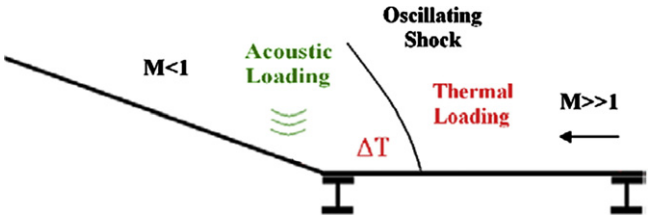

Fig. 2. Oscillating shock due to hypersonic flow over compression ramp.

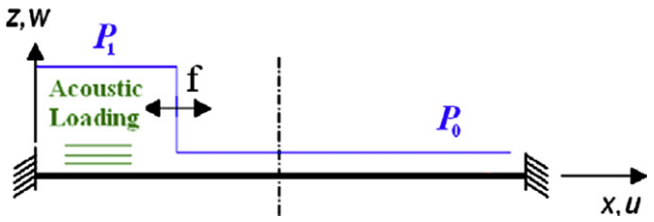

Fig. 3. Composite plate strip under time-varying spatial loading distribution.

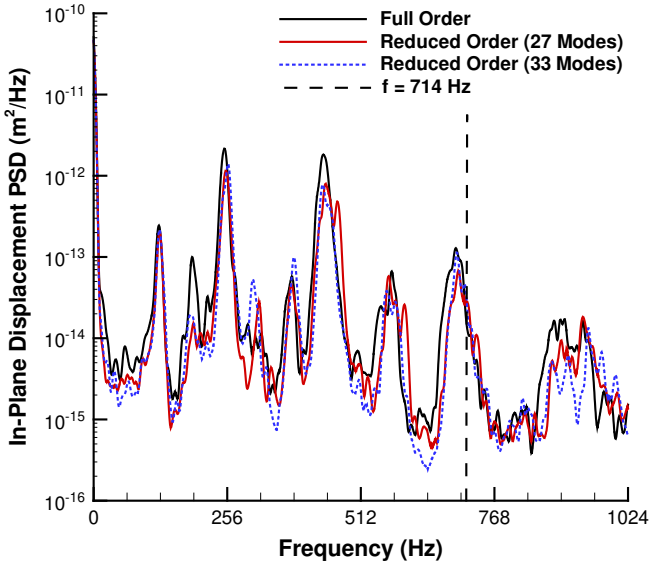

Fig. 4. In-plane displacement power spectral density (PSD) at the quarter-span location.

In the next example, the MAP approach (see Section 5.4) is utilized for basis selection and the concept of a cumulative basis is introduced. A condition representative of a hypersonic flight regime is presented in Fig. 2, where an oscillating shock formed ahead of a compression ramp is acting in a combined thermo-acoustic loading environment. Since the thermal loads are addressed with higher fidelity examples elsewhere in this review, a simplification adopted in this study [37] is shown in Fig. 3 where the oscillating boundary between high static pressure P_1 and low static pressure P_0 moves over a specified span with frequency f, while the acoustic disturbance propagates in the subsonic region aft of the shock. The structure considered in this study is a clamped–clamped composite plate strip. It is assumed that, representative of a typical hypersonic mission profile, excitation parameters vary slowly over the duration of the mission. Therefore, seven load cases were considered to characterize the variation in the span, frequency and location of the pressure discontinuity oscillations. As previously mentioned in Section 5.2, there is a computational incentive to develop a reduced order model capable of supporting analysis under a range of conditions. Consequently, the system identification and modal basis selection procedure using the MAP approach, see Section 5.4.1, was individually applied for all seven loading conditions. The union of the resulting seven basis sets was then taken to form a single cumulative basis set applicable across all loadings [37].

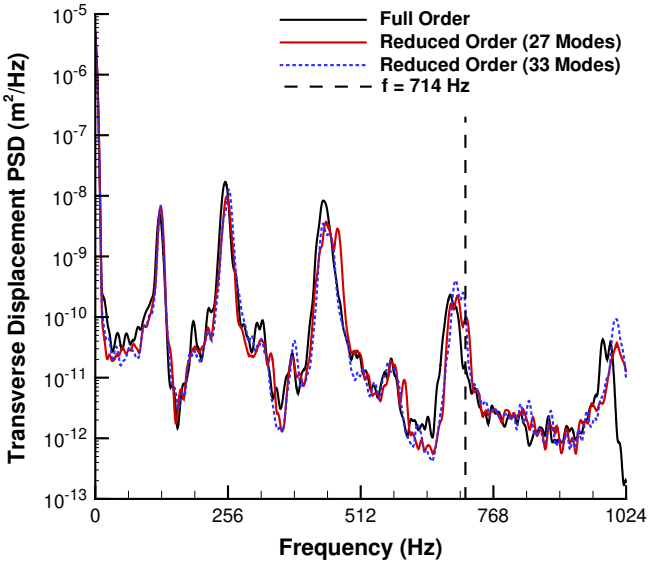

Fig. 5. Transverse displacement power spectral density (PSD) at the quarter-span location.

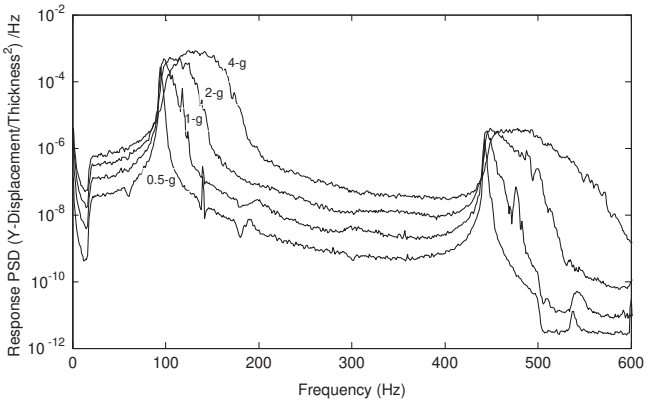

Fig. 6. Experimental clamped–clamped, flat beam mid-span response to inertial loading [0, 500 Hz].

Using the MAP approach, a single baseline excitation case resulted in selection of 27 linear modes, while the cumulative basis spanning all seven cases required 33 linear modes. Both reduced order systems produced results that compared very favorably with the simulation in physical degrees of freedom, as seen in Figs. 4 and 5. The cumulative basis system using 33 basis functions was formed by solving a total of 7139 nonlinear static cases per Eqs. (26)–(27). If individual reduced order systems were developed for each of seven loading variations, the total number of nonlinear static cases to be solved would increase by more than three-fold to 22,170. Note that the cumulative basis concept is particularly straightforward to apply when the basis functions identified across individual loading cases are load-independent and orthogonal.

The above two validations have been numerical, i.e. comparisons between reduced order and full order predictions. Ultimately though, it would be expected that the reduced order model predictions would match the measured response of physical structures, particularly for aircraft structural design purposes. ROMs will be used early in design, before structural components are built, to quickly predict response for time-dependent limit-state analyses and those predictions will be compared with actual structural testing [53]. What are needed are robust ROMs amenable to experimental-based model updating.

To perform such comparisons successfully, it is necessary that the experiment be well-characterized, i.e. that the physical properties of the experiment, including the boundary conditions, be extracted accurately enough so that the results can be replicated using a simple model. To demonstrate this perspective, one experiment, conducted with the intent to compare with ROMs, was undertaken in [54]. The displacement and strain response of a thin, clamped–clamped steel beam to several excitation levels (0.5–4 g inertial loading) and axial preloads was measured and documented. An idealized single degree of freedom beam model with estimated boundary conditions, linear and nonlinear parameters was

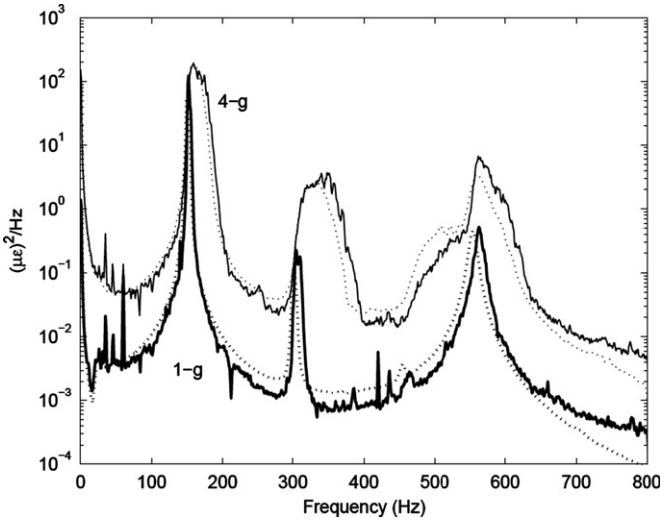

Fig. 7. Experiment (solid line) and IC strain predictions (dotted line) of thermally pre-loaded beam.

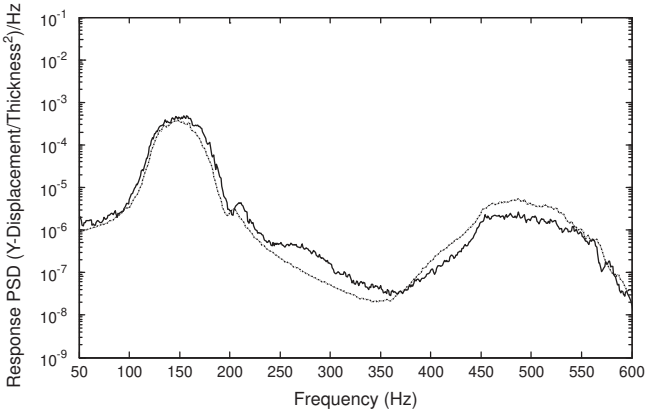

Fig. 8. Clamped–clamped beam quarter-point response to 9-g RMS inertial loading using experimentally derived linear and nonlinear parameters, [0, 500 Hz] (solid line: experiment response; dash–dot line: predicted response).

utilized. Fig. 6 shows the beam mid-span normalized deflections for several different load cases. The results demonstrate the geometrically nonlinear response typical of acoustic fatigue prone structures.

Several different ROM methods were applied to the finite element model representing the physical experiment [55] and were compared to the experimental results of Gordon et al. [54]. The comparisons are quite good between the IC method and experimental results as noted in Fig. 7. In an approach similar to the IC one, it was demonstrated that nonlinear ROMs can also be identified from experimental data [24]. In this approach, consistent response measurements were made along the length of a clamped–clamped beam similar to the one just described. A geometric nonlinear model with cubic only stiffness coefficients ($K^{(3)}_{ijlp}$) was assumed. By proceeding in this manner, the resulting in-plane displacements were implicitly condensed into the transverse displacement only model. The experimental results were filtered in the time domain, while the identification was accomplished in the frequency domain. The linear damping and frequencies components were identified using a rational fraction polynomial technique, while the cubic coefficients were identified in a least-squares sense. The method was demonstrated to be successful for this simple beam structure, as evidenced in Fig. 8, by the comparison of measured and predicted response for an excitation level much greater than that used for the identification of the model.

Further, the above studies have also demonstrated the effect of thermal pre-load and damping on the geometric nonlinear response. In the past, geometric nonlinearity for sonic fatigue type response has been attributed to damping. It was shown in [55] that an increase in damping, for a ROM system, will actually diminish the effect of the geometric nonlinearity. Also discussed, was the sensitivity of the ROM to the coefficients of the nonlinear stiffness terms.

7. Multidisciplinary applications

The prediction of the response of aircraft panels, of hypersonic vehicles especially, is not simply a structural issue as the panel interacts with the air surrounding it leading to a coupled aerothermoelastic problem, e.g. see [11], which is particularly challenging/time consuming to address in the context of full (e.g. finite element) models. However, as stated above, a key advantage of reduced order models is their simple form which permits their incorporation as a structural model in a multidisciplinary framework. This coupling capability has been exemplified in particular with aerodynamics (see Section 7.3) and acoustics (see Section 7.4). In these applications, the forces acting on the structure originate from the other discipline and depend on the response of the structure.

The coupling between thermal and structural problems is more intricate as restrained thermal expansions lead to stresses that affect the structural response. That is, the temperature appears directly in the parameters of the reduced order model (even if the elasticity tensor is assumed to be temperature independent) *as well as* a pseudo excitation (i.e. on the right-hand-side of Eq. (8)). This special coupling is described in detail in the next two sections, first (Section 7.1) in situations in which the temperature distribution (but maybe not the magnitude) is fixed and then (Section 7.2) in a coupled structural–thermal format in which both fields are modeled using reduced order models thereby allowing spatial and temporal variations of the temperature distribution.

Earlier discussions have emphasized the importance of the basis selection (see Section 5) for the fidelity of the structural reduced order model. This issue is especially important in the multidisciplinary applications considered here and can often be viewed as a two-step process.

To clarify the first step, referred to here as the "baseline structure" selection, recall that the basis functions of Section 5 are all structural responses (free or forced) and thus depend on the stress field preexisting on the structure because of its nonlinearity. The above first step is thus the specification of the constant loading, if any, applied to the structure during the determination of the basis functions. To clarify this issue, consider the response of a heated panel (with a constant temperature distribution) to time-varying forces and assume that the basis is to be built on linear modes (e.g. as in Sections 5.1–5.4). It then remains to decide whether these modes are of the heated panel (basis referred to as the "warm modes") or those of the unheated panel (the "cold modes"); this is the baseline structure selection. In fact, this issue is not specific to, albeit particularly acute in, multidisciplinary problems. For example, the response of a structure to a non-zero mean varying pressure could be approached using the modes of the unloaded structure or their counterparts for the structure subjected to the mean pressure distribution.

The second step of the basis selection process focuses on the detailed construction of the basis functions. Specifically, a first option is to select the structural basis functions without any information on the detailed form of the loading induced by the other discipline, relying only on, say, the expected frequency band of the response. A second approach consists of using some structural responses of the fully coupled problem to either "enrich" the first option basis or to build entirely the basis, e.g. in a POD format. In both of these situations, the structural ROM formulation is carried out independently of the treatment, i.e. full or reduced order modeling, of the other discipline(s). In some cases however, most notably when the other discipline is governed by linear equations, it is also possible to formulate a ROM of the *fully coupled* fields in which the structural and other discipline's bases are dependent of each other. To date, this approach appears to have been suggested only in connection with acoustic problems (the complex eigenvector approach of Section 7.4).

7.1. Thermoelastic problems—fixed temperature distribution

The formulation and validation of reduced order models of the structural response of heated panels has been the subject of a large number of investigations to date owing to both its practical importance (e.g. in the context of panels of hypersonic vehicles) and its complexity (e.g. occurrence of thermal buckling and snap through of buckled panels). In most of these investigations [31,36,38,48,55–57], the temperature distribution was prescribed, either fixed or scaled by an overall magnitude. The case of a panel of uniform temperature has been particularly extensively considered with the ROM parameters either computed at each temperature, using the indirect approaches of Sections 4.2 and 4.3, or selected to vary with temperature as shown in Section 7.2, i.e. with the linear stiffness terms varying linearly with temperature and the other parameters independent of it. In this latter scenario, the parameters are typically evaluated (as in Sections 4.2 and 4.3) at two different temperatures to fully characterize the temperature dependence of the linear stiffness coefficients.

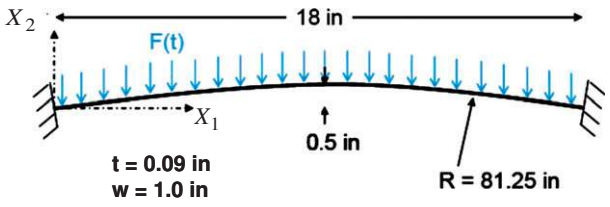

Fig. 9. Curved beam geometry.

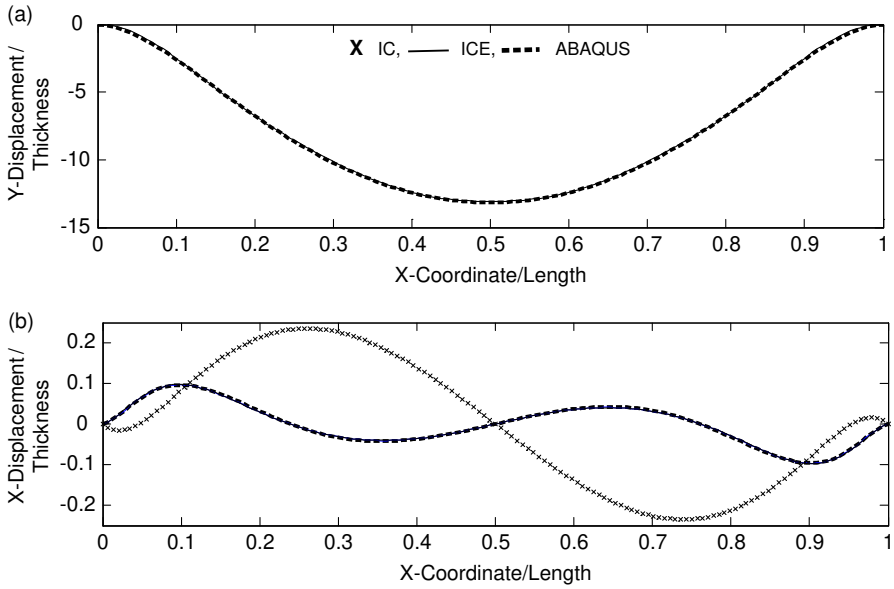

Fig. 10. IC, ICE and Abaqus (a) transverse and (b) in-plane deflections, $\Delta T = 150\ ^\circ$F.

The validation results presented in [31,36,38,48,55–57] confirm those obtained in the non-thermal case, e.g. see Section 6: an excellent agreement can be obtained over a broad range of temperature with both cold and hot modes. As an example of such validations, consider the curved beam of Fig. 9 (see [36] for details) the reduced order modeling of which was carried out by the IC and ICE methods (see Section 5.1) over a range of temperatures using the cold modes. Then, shown in Fig. 10 is the transverse (X_2) and in-plane (X_1) displacements predicted by both Abaqus and the IC and ICE methods due to a temperature increase of 150 °F and a uniform static pressure (in the X_2 direction) of 3 lb/in.

7.2. Thermoelastic problems—combined structural–thermal ROM

Focusing on future coupled aero-thermo-structural analyses, a recent investigation [58] proposed and validated a combined structural–thermal ROM approach in which the temperature field is represented in an expansion similar to Eq. (1), i.e. as

$$T(\mathbf{X},t) = \sum_{n=1}^{\mu} \tau_n(t)\, T^{(n)}(\mathbf{X}) \tag{54}$$

where $T^{(m)}$ are specified functions (the thermal basis functions) of the position vector $\mathbf{X}$ in the undeformed configuration. The derivation of the governing equations for the coupled structural–thermal ROM proceeds in parallel to the derivation of Section 3, with the field Eq. (2) complemented with the heat conduction equation

$$\rho_0\, T\, \dot{\mathcal{S}} = \frac{\partial}{\partial X_i}\left[k_{ij}^0 \frac{\partial T}{\partial X_j}\right] \tag{55}$$

where $\mathcal{S}$ denotes the specific entropy and $\mathbf{k}^0$denotes the conductivity tensor pulled back to the undeformed configuration.

The material constitutive equation to be introduced next will generalize Eq. (7) to include the temperature. It stems from the Helmholtz free energy (per unit mass) $\mathcal{F}$ defined as

$$\mathcal{F} = \mathcal{E} - T\mathcal{S} \tag{56}$$

where $\mathcal{E}$ denotes the elastic energy. Expressions for the 2nd Piola–Kirchhoff stress components and the entropy can then be derived as [17]

$$\rho_0\left(\frac{\partial \mathcal{F}}{\partial E_{ij}}\right)_T = S_{ij} \quad \text{and} \quad \left(\frac{\partial \mathcal{F}}{\partial T}\right)_{E_{ij}} = -\mathcal{S} \tag{57),(58}$$

In [58], a Duhamel–Neumann form of the Helmholtz free energy was assumed, i.e.

$$\rho_0\, \mathcal{F} = \frac{1}{2} C_{ijkl}\, E_{ij}\, E_{kl} - C_{ijkl}\, \alpha_{kl}(T - T_0) E_{ij} + f(T, T_0) \tag{59}$$

where $\boldsymbol{C}$ denotes the fourth order elasticity tensor, $\boldsymbol{\alpha}$ the second order tensor of thermal expansion, T_0 is the reference temperature, and [17]

$$f(T,T_0) = -\rho_0 C_v T_0 \left[\frac{T}{T_0}\ln\left(\frac{T}{T_0}\right) - \frac{T}{T_0} + 1\right] \tag{60}$$

in which C_v is the specific heat per unit mass measured in the state of constant strain. With the selection of Eq. (59), one obtains in particular the expected stress definition

$$S_{ij} = \rho_0 \left(\frac{\partial \mathcal{F}}{\partial E_{ij}}\right)_T = C_{ijkl}[E_{kl} - \alpha_{kl}(T - T_0)]. \tag{61}$$

The derivation of the governing equations for the generalized coordinates $q_n(t)$ and $\tau_n(t)$ is then achieved by combining the above relations and proceeding with a Galerkin approach as carried out in Section 3. Assuming the material properties to be temperature independent, this process leads to the reduced order model equations (see [58] for definition of coefficients and [27] for an extension to tensor of elasticity and coefficient of thermal expansion varying linearly with the local temperature)

$$M_{ij}\ddot{q}_j + D_{ij}\dot{q}_j + K^{(1)}_{ij} q_j - K^{(th)}_{ijl} q_j \tau_l + K^{(2)}_{ijl} q_j q_l + K^{(3)}_{ijlp} q_j q_l q_p = F_i + F^{(th)}_{il}\tau_l \tag{62}$$

and

$$B_{ij}\dot{\tau}_j + \tilde{K}_{ij}\tau_j + K^{(st)}_{ijl}\tau_j \dot{q}_l = P_i + R_{ij}\tau_j. \tag{63}$$

Considering first the structural ROM equation, Eq. (62), note that temperature appears in two terms. As expected from Section 7.1, it only affects the linear stiffness terms and does so linearly. Next, Eq. (63) is the heat conduction equation in which B_{ij} and $\tilde{K}_{ij}$ are the elements of the capacitance and conductance matrices of the reduced order model while the coupling term $K^{(st)}_{ijl}\tau_j\dot{q}_l$ is recognized as the latency effect. Finally, P_i denotes the source term associated with the boundary conditions (e.g. heat flux applied from aerodynamics) while R_{ij} originates from the difference between the conductivity tensor $\mathbf{k}$ and its pulled back (see [17]) counterpart $\mathbf{k}^0$ and thus is a deformation dependent term. These observations demonstrate that Eqs. (62) and (63) are fully (2-way) coupled. Note however that the latency effect and the term R_{ij} are both typically small (see discussion in [58]) and thus could be neglected leading to a one-way coupling only, the temperature affecting the structural response.

The identification of the new coefficients appearing in Eqs. (62) and (63) has been accomplished as an extension of the methods discussed in Section 4.2 (see [58]) and the approach has been applied to a series of problems [27,58–60] including thermal loading only (steady and unsteady) or combined with a random acoustic excitation (again both steady and unsteady thermal loading). The validation of the methodology was carried out by comparing both structural and thermal predictions.

As an example, shown in Fig. 11(a) is a panel (modeled by a beam) subjected to a heat flux of constant, triangular distribution of width 2Δ which oscillates about the fixed position a_0 (taken as half of the beam length in the numerical computations). Both structural and thermal ROM were developed for this problem with 14 thermal basis functions based on eigenvectors of the generalized eigenvalue problem formed by the capacitance and conductance matrices with a combined linear and cubic (see [58,59] for details) dependence through thickness. The structural basis was developed with the baseline structure being unheated (since the mean temperature distribution could not be directly determined) and unloaded. Then, the first 7 transverse modes of this baseline beam were selected first. Next, 7-dual modes with mode 1 dominant (see Section 5.3) were introduced to model the nonlinear transverse-in-plane coupling. Finally, the basis was enriched with the first three in-plane linear modes to account for the in-plane thermal displacements induced by the unknown mean heat flux. The structural model thus included 17 modes. Shown in Fig. 11(b)–(d) are comparisons of the temperatures and in-plane and transverse displacements predicted over a period of the flux oscillation by the combined ROM and Nastran. With regard to these results, note that Nastran does not have an option to proceed with the joint thermal-structural analysis and thus the structural results were predicted using the same temperature distribution as the ROM.

7.3. Aeroelastic applications

Aeroelastic analyses are traditionally conducted under the assumption that the structure is linear and thus its response is represented in a modal form. A classic departure from this assumption is the treatment of panel flutter in which the geometric nonlinearity must be accounted for. Reduced order models are particularly well suited for this application. For example, to study the panel flutter phenomenon with a linear aerodynamic model (e.g. the first-order piston theory), the equation of motion in physical coordinates, Eq. (10), needs to be modified by adding aerodynamic influence matrices (damping and stiffness), and eliminating the excitation vector from the right-hand-side [61–63]. The system can be then transformed to modal coordinates using two distinct strategies.

Initially, Abdel-Motagaly et al. [61] used in vacuo linear modes $\hat{\boldsymbol{\Phi}}_r$ in the process of modal transformation. With this type of basis, six linear modes were needed to obtain converged limit cycle oscillations (LCO) when isotropic or orthotropic

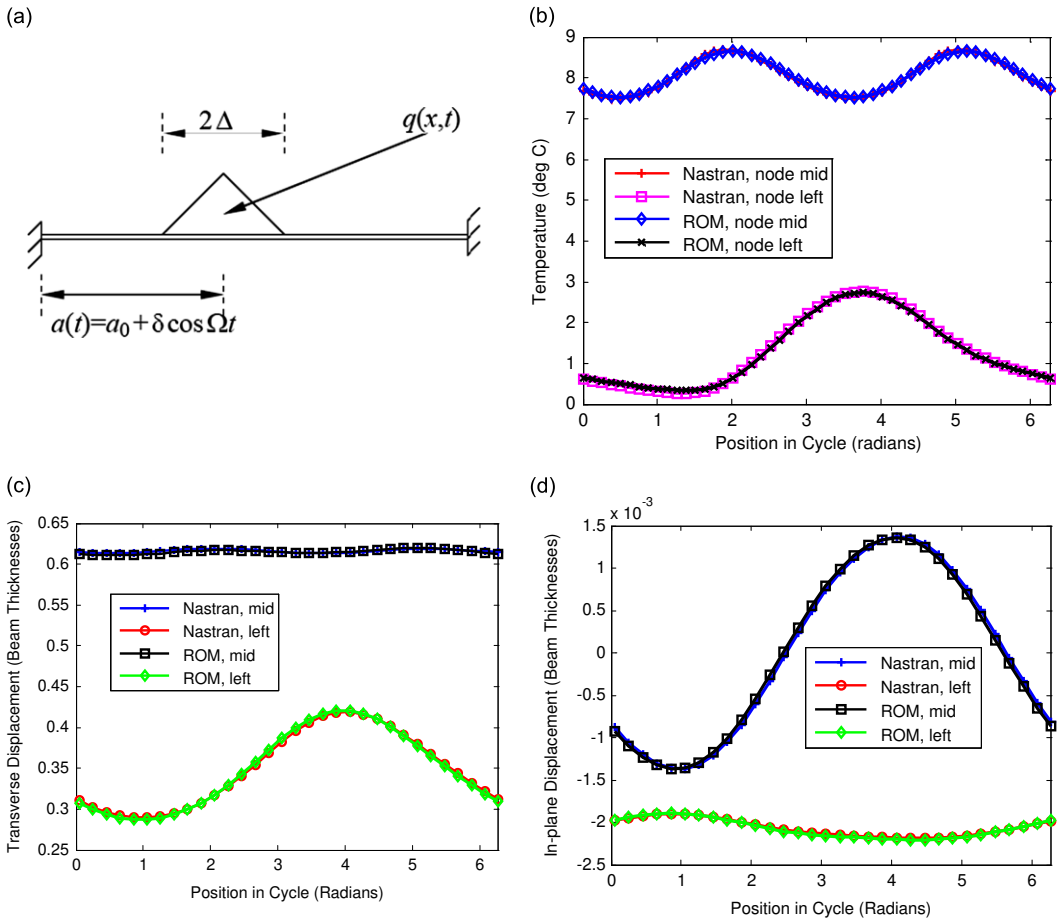

Fig. 11. (a) Oscillating flux on panel. Time history of (b) temperature, (c) transverse and (d) in-plane deflections at the beam middle and at a node near the furthest left excursion of the flux, $\Omega = 160\pi$ (80 Hz). Nastran and ROM computations.

rectangular plates were studied at zero yaw angle. An anisotropic plate required more than six linear modes at the same zero flow angle. For an arbitrary flow angle all panels required 36 such modes for the LCO convergence.

The large number of linear modes needed for the LCO convergence motivated Guo and Mei [62] to propose using the so-called aero-elastic modes (AEMs). AEMs are obtained from a pre-stressed eigenvalue problem, where the pre-load is due to the steady aerodynamic loading. In effect, the baseline structure (see discussion above) is then the aerodynamically pre-loaded panel. The authors demonstrated that using AEMs leads to a very significant reduction in the number of basis functions required for a converged LCO solution to two for the zero yaw angle study cases and six to seven AEMs for the arbitrary angle study cases regardless whether the panel considered was isotropic, orthotropic, or anisotropic.

While the above studies were conducted on flat panels in ambient temperature, the approach was recently generalized by Ghoman et al. [64] to shallowly curved panels under the combined elevated temperature environment and arbitrary flow angle.

Furthermore, for flat panel study cases, both linear modes- and AEMs-based reduced order system formulations were successfully used to study suppression of panel flutter at elevated temperatures by using shape memory allows (SMAs) [56,65]. Moreover both linear modes and AEMs-based simulations were applied to study active control of panel flutter using piezoelectric actuators [66,67].

The application of nonlinear geometric reduced order models in aeroelastic applications is not limited to panel flutter. In addition, structural reduced order models such as the ones reviewed here can be coupled to full order or reduced order models (e.g. see [68–76]) of the aerodynamics. Such a coupling has in fact been accomplished [15,68,77] and the combination of structural and aerodynamic ROMs has been found to be extremely computationally efficient while capturing the nonlinearity in both flow and structural behavior.

7.4. Structural–acoustic coupling

Sonic fatigue prone structures and advanced structural concepts intended for hypersonic, space-access, or low-observable, buried engine extreme environments, are often tested in progressive wave-tube facilities. Although a subset of

the actual environment, i.e., minimal flow velocities (the bulk flow is a byproduct of the noise generators) and lower frequency cutoffs (a function of the noise generators and duct geometry), these facilities recreate significant combined thermal and fluctuating pressure environments that are relevant to air-vehicle structural response and fatigue. In these test facilities, compressed air is forced through a number of valves that are opened and closed at random intervals. The random signal used to control the valves is filtered and shaped to match the broad-band frequency content typical of aircraft engine noise. The resulting acoustic waves propagate down the tunnel and through the test-section . One wall of the tunnel test-section consists of the structural panel of interest. The test panels are mounted on a testing rig, isolated from the progressive tunnel. So, although the panel makes up a wall of the test-section, the panel is not in direct contact with the facility. The grazing incidence pressure waves, typically of high-intensity for sonic fatigue testing, excite the panel vibration modes of interest resulting in multimode nonlinear response and fatigue. Both the Air Force and NASA maintain such facilities. During recent testing in the Air Force progressive wave facilities, it was observed that the acoustic modes of the facility were close in frequency to the natural frequencies of the test article in question [78]. As a result, an innovative method was developed coupling structural ROMs with an acoustic reduced order model, and the derivation is repeated here briefly for completeness. The coupled (displacement and pressure) linear structural and acoustic finite element equations of motion can be expressed as

$$\begin{bmatrix} \mathbf{M}_s & 0 \\ \rho\mathbf{S} & \mathbf{M}_a \end{bmatrix} \begin{bmatrix} \ddot{\mathbf{y}} \\ \ddot{\mathbf{p}} \end{bmatrix} + \begin{bmatrix} \mathbf{C}_s & 0 \\ 0 & \mathbf{C}_a \end{bmatrix} \begin{bmatrix} \dot{\mathbf{y}} \\ \dot{\mathbf{p}} \end{bmatrix} + \begin{bmatrix} \mathbf{K}_s & -\mathbf{S}^T \\ 0 & \mathbf{K}_a \end{bmatrix} \begin{bmatrix} \mathbf{y} \\ \mathbf{p} \end{bmatrix} = \begin{bmatrix} \mathbf{f}_s \\ \mathbf{f}_a \end{bmatrix}, \tag{64}$$

where $\mathbf{M}_s$ is the structural mass matrix, $\mathbf{M}_a$ is the acoustic mass matrix, $\mathbf{S}$ is a structural–acoustic coupling matrix, ρ is the fluid density, $\mathbf{y}$ is the displacement vector, $\mathbf{p}$ is the pressure vector, $\mathbf{f}_s$is the structural force vector, and $\mathbf{f}_a$ is the acoustic force vector [79,80].

A first approach to obtain a reduced order model of the structural–acoustic system is to adopt a set of domain-specific basis vectors for acoustic and structural domains, i.e.

$$\begin{Bmatrix} \mathbf{w} \\ \mathbf{p} \end{Bmatrix} = \begin{bmatrix} \Phi & 0 \\ 0 & \Psi \end{bmatrix} \begin{Bmatrix} \mathbf{q} \\ \mathbf{a} \end{Bmatrix}, \tag{65}$$

where $\Phi = [\boldsymbol{\varphi}^{(1)}\boldsymbol{\varphi}^{(2)}\ldots\boldsymbol{\varphi}^{(M)}]$ is the structural basis (see Section 5 for discussion) and Ψ is its counterpart for the acoustic domain, and $\mathbf{q}$ and $\mathbf{a}$ are the vectors of structural and acoustic generalized coordinates. The resulting governing equations for the former set of coordinates is given by Eq. (8) with

$$\mathbf{F} = \mathbf{E}^{\mathrm{T}}\mathbf{a} + \Phi^{\mathrm{T}}\mathbf{f}_s \quad \text{where } \mathbf{E} = \Psi^{\mathrm{T}}\mathbf{S}\Phi. \tag{66}$$

Further, the modal acoustic equations are

$$\ddot{\mathbf{a}} + \tilde{\mathbf{C}}_a\dot{\mathbf{a}} + \tilde{\mathbf{K}}_a\mathbf{a} = -\rho\mathbf{E}\ddot{\mathbf{q}} + \Psi^{\mathrm{T}}\mathbf{f}_a \tag{67}$$

where

$$\tilde{\mathbf{C}}_a = \psi^T\mathbf{C}_a\psi \quad \text{and} \quad \tilde{\mathbf{K}}_a = \psi^T\mathbf{K}_a\psi. \tag{68}$$

The nuances and the detailed steps of these approaches are described in much greater detail in [79]. Results of this coupled structural–acoustic modeling method in [78,81] demonstrate the efficacy of the method. In this comparison, a

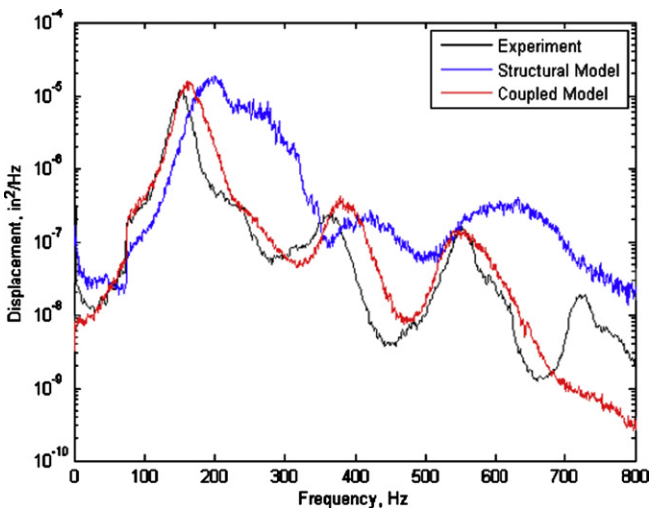

Fig. 12. Structure-only and structural–acoustic reduced order model predictions versus experimental progressive wave facility measured displacements.

structural-only and the structural–acoustic coupled model were compared with the measured displacement response of an adhesively bonded flat panel in the Air Force Research Laboratory progressive wave facility, see Fig. 12.

The coupled structural–acoustic of Eq. (65)–(68) reduced order model is seen to capture well the response of this thin-gauge panel in a complex loading environment. Note finally that another approach investigated in [82] is based on a reduced order modeling of the coupled structural and acoustic equations, i.e. the complex eigenvectors associated with the left-hand-side of Eq. (64). While physically appealing, this approach is much more complex than the one described above (from [79]) but it provides a direct estimate of the acoustically induced dissipation.

8. Conclusions

This paper presented an extensive review of indirect methods for the construction of reduced order models for the prediction of the response of geometrically nonlinear structures modeled by finite element models. The term indirect is used here to indicate that only standard output results of the finite element computations are used, i.e. no detailed information on the elements formulation is assumed. Accordingly, these methods are suitable to use with commercial finite element software such as Nastran, Abaqus, etc.

The reduced order models considered here are parametric in that the form of the governing equations for the model's generalized coordinates is known. In fact, it was shown (see Section 3) to be nonlinear only in the stiffness terms which are full cubic polynomials of these coordinates. The indirect identification of the parameters of these polynomials from static nonlinear finite element analyses was addressed next and two methods were reviewed that rely on the specification of either displacements (Section 4.2) or forces (Section 4.3) and the finite element computation of the other.

A key element in the reduced order modeling effort is the selection of the basis to represent the motion and three different strategies (see Sections 5.1, 5.3, and 5.4) are accordingly reviewed that rely heavily, although not completely, on the linear modes of the structure. Each one has its own advantages/merits in terms of number of basis functions used, accuracy in representing the response, and complexity in obtaining the basis. A sample of existing validation cases then demonstrated the high accuracy that can be obtained with these reduced order models even in the presence of strong geometric nonlinearity and further suggests that each of the three basis selection strategy can be used successfully.

Reduced order models are particularly useful in multidisciplinary analyses, not only because of the reduction in computational effort they imply but also because they are typically more easily coupled to other disciplinary codes than full finite element models. Accordingly, the final part of this review focused on such multidisciplinary applications, more specifically on the coupling/interaction with the temperature distribution, aerodynamics, and acoustics, all of which are important in key applications such as the sonic fatigue of hypersonic vehicles.

References

[1] R.D. Blevins, I. Holehouse, K.R. Wentz, Thermoacoustic loads and fatigue of hypersonic vehicle skin panels, *Journal of Aircraft* 30 (1993) 971–978.
[2] P. Pozefsky, R.D. Blevins, A.L. Laganelli, Thermo-vibro-acoustic loads and fatigue of hypersonic flight vehicle structure, Technical Report AFWAL-TR-89-3014, Flight Dynamics Laboratory, Air Force Research Laboratory, 1989.
[3] B.L. Clarkson, Review of sonic fatigue technology, *NASA* (1994). CR-4587.
[4] R.D. Blevins, An approximate method for sonic fatigue analysis of plates and shells, *Journal of Sound and Vibration* 129 (1989) 51–71.
[5] J.J. Hollkamp, R.W. Gordon, Modeling membrane displacements in the sonic fatigue response prediction problem, *Proceedings of the 46th Structures, Structural Dynamics, and Materials Conference*, Austin, Texas, AIAA-2005-2095, April 2005.
[6] M. Morton, Certification of the F-22 advanced tactical fighter for high cycle and sonic fatigue, *Proceedings of the 48th Structures, Structural Dynamics, and Materials Conference*, Honolulu, Hawaii, AIAA-2007-1766, April 2007.
[7] J.W. Miles, On structural fatigue under random loading, *Journal of the Aeronautical Sciences* 21 (1954) 753–762.
[8] F. Rudder, H. Plumblee, Sonic fatigue design guide for military aircraft, US Air Force Technical Report AFFDL-TR-74-112, 1975.
[9] W.K. Chiu, U. Siovitz, S.C. Galea, L.L. Koss, Life extension of acoustically fatigued panels using add-on dampers, *Computers and Structures* 44 (1999) 179–188.
[10] J. Coate, P. Meltzer, AFRL examines technology used to test B-2 aft deck performance, 〈http://www.wpafb.af.mil/news/story.asp?id=12310405〉, 2009.
[11] A. Culler, J. McNamara, Coupled flow–thermal–structural analysis for response prediction of hypersonic vehicle skin panels, *Proceedings of the 51st Structures, Structural Dynamics, and Materials Conference*, Orlando, Florida, AIAA-2010-2965, April 2010.
[12] C. Ostoich, D.J. Bodony, P.H. Geubelle, Coupled fluid–thermal response of a spherical dome due to a Mach 6.59 laminar boundary layer, *AIAA Journal* 50 (12) (2012) 2791–2808.
[13] E.L. Blades, R.S. Miskovish, M. Nucci, P. Shah, P.G. Bremner, E.A. Luke, Towards a coupled mutliphysics analysis capability for hypersonic vehicle structures, *Proceedings of the 52nd Structures, Structural Dynamics and Materials Conference*, Denver, Colorado, AIAA-2011-1962, April 2011.
[14] K. Kim, V. Khanna, X.Q. Wang, M.P. Mignolet, Nonlinear reduced order modeling of flat cantilevered structures, *Proceedings of the 50th Structures, Structural Dynamics, and Materials Conference*, Palm Springs, California, AIAA-2009-2492, May 2009.
[15] Z. Wang, S. Yang, D.D. Liu, X.Q. Wang, M.P. Mignolet, R.E. Bartels, Nonlinear aeroelastic analysis for a wrinkling aeroshell/ballute system, *Proceedings of the 51st Structures, Structural Dynamics, and Materials Conference*, Orlando, Florida, AIAA-2010-2879, April 2010.
[16] Y.-W. Chang, X.Q. Wang, E. Capiez-Lernout, M.P. Mignolet, C. Soize, Reduced order modeling for the nonlinear geometric response of some curved structures, *Proceedings of the 2011 International Forum of Aeroelasticity and Structural Dynamics*, Paris, France, IFASD-2011-185, June 2011.
[17] Y.C. Fung, P. Tong, *Classical and Computational Solid Mechanics*, World Scientific, River Edge, New Jersey, 2001.
[18] J. Bonet, R.D. Wood, *Nonlinear Continuum Mechanics for Finite Element Analysis*, Cambridge University Press, Cambridge, 1997.
[19] M.P. Mignolet, C. Soize, Stochastic reduced order models for uncertain geometrically nonlinear dynamical systems, *Computer Methods in Applied Mechanics and Engineering* 197 (2008) 3951–3963.
[20] S.A. Rizzi, A. Przekop, The effect of basis selection on static and random acoustic response prediction using a nonlinear modal simulation, NASA/TP-2005-213943, 2005.
[21] M. Azzouz, X. Guo, A. Przekop, C. Mei, Comparison of PDE/Galerkin and FEM for nonlinear aerospace structures analyses, *Proceedings of the 44th Structures, Structural Dynamics and Materials Conference*, Norfolk, Virginia, AIAA-2003-1856, April 2003.

[22] C. Mei, Three decades' interesting experience in nonlinear finite element formulation development and aerospace applications, *Proceedings of Eighth International Conference on Recent Advances in Structural Dynamics*, Southampton, July 2003.
[23] A. Przekop, M.S. Azzouz, X. Guo, C. Mei, L. Azrar, Finite element multiple-mode approach to nonlinear free vibrations of shallow shells, *AIAA Journal* 42 (2004) 2373–2381.
[24] S.M. Spottswood, R.J. Allemang, On the investigation of some parameter identification and experimental modal filtering issues for nonlinear reduced order models, *Experimental Mechanics* 47 (2007) 511–521. 47.
[25] A.A. Muravyov, S.A. Rizzi, Determination of nonlinear stiffness with application to random vibration of geometrically nonlinear structures, *Computers and Structures* 81 (2003) 1513–1523.
[26] K. Kim, A.G. Radu, X.Q. Wang, M.P. Mignolet, Nonlinear reduced order modeling of isotropic and functionally graded plates, *International Journal of Non-Linear Mechanics* 49 (2013) 100–110.
[27] A. Matney, S.M. Spottswood, M.P. Mignolet, Nonlinear structural reduced order modeling methods for hypersonic structures, *Proceedings of the 53rd Structures, Structural Dynamics and Materials Conference*, Honolulu, Hawaii, AIAA-2012-1972, April 2012.
[28] M. Nash, Nonlinear Structural Dynamics by Finite Element Modal Synthesis, PhD Dissertation, Department of Aeronautics, Imperial College, The University of London, London, UK, 1977.
[29] M.I. McEwan, J.R. Wright, J.E. Cooper, A.Y.T. Leung, A finite element/modal technique for nonlinear plate and stiffened panel response prediction, *Proceedings of the 42nd Structures, Structural Dynamics, and Materials Conference*, Seattle, Washington, AIAA-2001-1595, April 2001.
[30] J.J. Hollkamp, R.W. Gordon, S.M. Spottswood, Nonlinear modal models for sonic fatigue response prediction: a comparison of methods, *Journal of Sound and Vibration* 284 (2005) 1145–1163.
[31] R.W. Gordon, J.J. Hollkamp, Reduced-order models for acoustic response prediction, Air Force Research Laboratory Report AFRL-RB-WP-TR-2011-3040, 2011.
[32] D.J. Inman, *Vibration: With Control, Measurement, and Stability*, Prentice-Hall, Inc. Englewood Cliffs, New Jersey, 1989.
[33] R. Ohayon, C. Soize, *Structural Acoustics and Vibration*, Academic Press, London, 1998.
[34] Y. Shi, C. Mei, A finite element time domain modal formulation for large amplitude free vibrations of beams and plates, *Journal of Sound and Vibration* 193 (1996) 453–464.
[35] R.W. Gordon, J.J. Hollkamp, Reduced-order modeling of the random response of curved beams using implicit condensation, *Proceedings of the 47th Structures, Structural Dynamics, and Materials Conference*, Newport, Rhode Island, AIAA-2006-1926, May 2006.
[36] S.M. Spottswood, T.G. Eason, X.Q. Wang, M.P. Mignolet, Nonlinear reduced order modeling of curved beams: a comparison of methods, *Proceedings of the 50th Structures, Structural Dynamics, and Materials Conference*, Palm Springs, California, AIAA-2009-2433, May 2009.
[37] A. Przekop, S.A. Rizzi, Nonlinear reduced-order analysis with time-varying spatial loading distributions, *Journal of Aircraft* 46 (2009) 1395–1402.
[38] A. Przekop, S.A. Rizzi, Dynamic snap-through of thin-walled structures by a reduced-order method, *AIAA Journal* 45 (2007) 2510–2519.
[39] A. Przekop, S.A. Rizzi, Nonlinear reduced order finite element analysis of structures with shallow curvature, *AIAA Journal* 44 (2006) 1767–1778.
[40] X.Q. Wang, Z. Wang, M.P. Mignolet, Reduced order modeling of the geometrically nonlinear response of a wrinkled ballute, *Proceedings of the 5th International Conference on Advanced Computational Methods in Engineering (ACOMEN 2011)*, Liege, Belgium, November 2011.
[41] P. Tiso, E. Jansen, M. Abdalla, Reduction method for finite element nonlinear dynamic analysis of shells, *AIAA Journal* 49 (2011) 2295–2304.
[42] E. Pesheck, C. Pierre, S.W. Shaw, Modal reduction of a nonlinear rotating beam through nonlinear normal modes, *Journal of Vibration and Acoustics* 124 (2002) 229–236.
[43] B.F. Feeny, R. Kappagantu, On the physical interpretation of proper orthogonal modes in vibrations, *Journal of Sound and Vibration* 211 (1998) 607–616.
[44] B.F. Feeny, Y. Liang, Interpreting proper orthogonal modes of randomly excited vibration system, *Journal of Sound and Vibration* 265 (2003) 953–966.
[45] D. Chelidze, W. Zhou, Smooth orthogonal decomposition-based vibration mode identification, *Journal of Sound and Vibration* 292 (2006) 461–473.
[46] S.A. Rizzi, A. Przekop, Nonlinear reduced-order simulation using an experimentally guided modal basis, *Proceedings of the 53rd Structures, Structural Dynamics and Materials Conference*, Honolulu, Hawaii, AIAA-2012-1971, April 2012.
[47] S.A. Rizzi, A. Przekop, POD/MAC-based modal basis selection for a reduced order nonlinear response analysis, *EUROMECH Colloquium 483—Geometrically Non-linear Vibrations of Structures*, Porto, Portugal, July 2007, pp. 101–104.
[48] S.A. Rizzi, A. Przekop, System identification-guided basis selection for reduced-order nonlinear response analysis, *Journal of Sound and Vibration* 315 (2008) 467–485.
[49] A. Przekop, S.A. Rizzi, An efficient modal basis selection criteria for reduced-order nonlinear simulation, *Proceedings of the 7th European Conference on Structural Dynamics EURODYN 2008, Southampton*, UK, Paper E69, July 2008.
[50] X. Guo, A. Przekop, Energy-based modal basis selection procedure for reduced-order nonlinear simulation, *Proceedings of 51st Structures, Structural Dynamics and Materials Conference*, Orlando, FL, AIAA-2010-2796, April 2010.
[51] U. Farooq, B.F. Feeny, Smooth orthogonal decomposition for modal analysis of randomly excited systems, *Journal of Sound and Vibration* 316 (2008) 137–146.
[52] A. Przekop, X. Guo, S.A. Rizzi, Alternative modal basis selection procedures for nonlinear random response simulation, *Journal of Sound and Vibration* 331 (2012) 4005–4024.
[53] S.L. Liguore, D.M. Pitt, M.J. Thomas, N. Gurtowski, Nonlinear, low-order/reduced-order modeling applications and demonstration, Report AFRL-RB-WP-TR-2011-3102, 2011.
[54] R.W. Gordon, J.J. Hollkamp, S.M. Spottswood, Nonlinear response of a clamped–clamped beam to random base excitation, *Proceedings of the Eighth International Conference on Recent Advances in Structural Dynamic*s, Southampton, UK, July 2003.
[55] J.J. Hollkamp, R.W. Gordon, S.M. Spottswood, Nonlinear sonic fatigue response prediction from finite element modal models: a comparison with experiments, *Proceedings of the 44th Structures, Structural Dynamics, and Materials Conference*, Norfolk, Virginia, AIAA-2003-1709, April 2003.
[56] X. Guo, A. Przekop, C. Mei, Supersonic panel flutter analysis and suppression using aeroelastic modes and shape memory alloys, *Proceedings of the 50th Structures, Structural Dynamics and Materials Conference*, Austin, Texas, AIAA-2005-2372, April 2005.
[57] S.M. Spottswood, J.J. Hollkamp, T. Eason, On the use of reduced-order models for a shallow curved beam under combined loading, *Proceedings of the 49th Structures, Structural Dynamics and Materials Conference*, Schaumburg, Illinois, AIAA-2008-2235, April 2008.
[58] R. Perez, X.Q. Wang, M.P. Mignolet, Nonlinear reduced order models for thermoelastodynamic response of isotropic and FGM panels, *AIAA Journal* 49 (2011) 630–641.
[59] R. Perez, X.Q. Wang, M.P. Mignolet, Steady and unsteady nonlinear thermoelastodynamic response of panels by reduced order models, *Proceedings of the 51st Structures, Structural Dynamics, and Materials Conference*, Orlando, Florida, AIAA-2010-2724, April 2010.
[60] A. Matney, R. Perez, M.P. Mignolet, Nonlinear unsteady thermoelastodynamic response of a panel subjected to an oscillating flux by reduced order models, *Proceedings of the 52nd Structures, Structural Dynamics and Materials Conference*, Denver, Colorado, AIAA 2011-2016, April 2011.
[61] K. Abdel-Motagaly, R. Chen, C. Mei, Nonlinear flutter of composite panels under yawed supersonic flow using finite elements, *AIAA Journal* 37 (1999) 1025–1032.
[62] X. Guo, C. Mei, Using aeroelastic modes for nonlinear panel flutter at arbitrary supersonic yawed angle, *AIAA Journal* 41 (2003) 272–279.
[63] K. Kim, Y.C. Kim, M.P. Mignolet, D.D. Liu, P.C. Chen, D.H. Lee, Random aeroelastic response due to strong hypersonic unsteady-wave/shock interaction with acoustic loads, *Proceedings of the 48th Structures, Structural Dynamics, and Materials Conference*, Honolulu, Hawaii, AIAA-2007-2014, April 2007.
[64] S. Ghoman, M. Azzouz, C. Mei, Time domain method for nonlinear flutter of curved panels under yawed supersonic flow at elevated temperatures, *Proceedings of the 50th Structures, Structural Dynamics and Materials Conference*, Palm Springs, California, AIAA-2009-2598, May 2009.
[65] B. Duan, K. Abdel-Motagaly, X. Guo, C. Mei, Flutter and thermal deflection suppression of composite plates using shape memory alloy, *AIAA Journal* 43 (2005) 2015–2023.

[66] K. Abdel-Motagaly, X. Guo, B. Duan, C. Mei, Active control of nonlinear panel flutter under yawed supersonic flow, *AIAA Journal* 43 (2005) 671–690.
[67] M. Kim, Q. Li, J.-K. Huang, C. Mei, Active control of nonlinear panel flutter using aeroelastic modes and piezoelectric actuators, *AIAA Journal* 46 (2008) 733–743.
[68] Z. Wang, D.D. Liu, P.C. Chen, S. Yang, Z. Zhang, M.P. Mignolet, X.Q. Wang, An expedient aeroelastic ROM-ROM methodology for nonlinear aerodynamic-nonlinear structural interactions (NANSI), *Proceedings of the 2009 International Forum on Aeroelasticity and Structural Dynamics (IFASD 2009)*, Seattle, Washington, IFASD-2009-010, June 2009.
[69] W.A. Silva, Application of nonlinear systems theory to transonic unsteady aerodynamic responses, *Journal of Aircraft* 30 (1993) 660–668.
[70] R.J. Prazenica, A.J. Kurdila, W. Silva, Multiresolution methods for representation of Volterra series and dynamical systems, *Proceedings of the 41st Structures, Structural Dynamics and Materials Conference*, Atlanta, Georgia, AIAA-2000-1754, April 2000.
[71] R.J. Prazenica, R. Lind, A.J. Kurdila, Uncertainty estimation from Volterra kernels for robust flutter analysis, *Proceedings of the 43rd Structures, Structural Dynamics and Materials Conference*, Denver, Colorado, AIAA-2002-1650, April 2002.
[72] T.J. Cowan, A.S. Arena Jr., K.K. Gupta, Accelerating computational fluid dynamics based aeroelastic predictions using system identification, *Journal of Aircraft* 38 (2001) 81–87.
[73] D.E. Raveh, Identification of CFD-based unsteady aerodynamic models for aeroelastic analysis, *Proceedings of the 44th Structures, Structural Dynamics and Materials Conference*, Norfolk, Virginia, AIAA-2003-1407, April 2003.
[74] K.L. Lai, K.S. Won, E.P.C. Koh, H.M. Tsai, Flutter simulation and prediction with CFD-based reduced-order model, *Proceedings of the 47th Structures, Structural Dynamics and Materials Conference*, Newport, Rhode Island, , AIAA-2006-2026, May 2006.
[75] D.J. Lucia, P.S. Beran, W.A. Silva, Aeroelastic system development using proper orthogonal decomposition and Volterra theory, *Proceedings of the 44th Structures, Structural Dynamics and Materials Conference*, Norfolk, Virginia, AIAA-2003-1922, April 2003.
[76] T. Kim, J.E. Bussoletti, An optimal reduced-order aeroelastic modeling based on a response-based modal analysis of unsteady CFD models, *Proceedings of the 42nd Structures, Structural Dynamics and Materials Conference*, Seattle, Washington, AIAA-2001-1525, April 2001.
[77] D.D. Liu, P.C. Chen, Z. Zhang, Z. Wang, S. Yang, D.H. Lee, M.P. Mignolet, K. Kim, F. Liu, N. Lindsley, P. Beran, Continuous dynamic simulation of nonlinear aerodynamic/nonlinear structure interaction (NANSI) for morphing wing aeroelasticity, *Proceedings of the 50th Structures, Structural Dynamics, and Materials Conference, Palm Springs, California*, AIAA-2009-2572, May 2009.
[78] J.J. Hollkamp, R. Gordon, T. Beberniss, Coupling acoustics to nonlinear structural models: predictions and experiments, *Proceedings of the 51st Structures, Structural Dynamics, and Materials Conference*, Orlando, Florida, AIAA-2010-2544, April 2010.
[79] J.J. Hollkamp, R. Gordon, Coupling acoustic modal models to nonlinear structural reduced- order models, *Proceedings of the 51st Structures, Structural Dynamics, and Materials Conference*, Orlando, Florida, AIAA-2010-2542, April 2010.
[80] H.J.-P. Morand, R. Ohayon, *Fluid–Structure Interaction: Applied Numerical Methods*, Wiley, 1995.
[81] J.J. Hollkamp, R.W. Gordon, The importance of structural–acoustic coupling in progressive wave testing, *Proceedings of the 52nd Structures, Structural Dynamics and Materials Conference*, Denver, Colorado, AIAA-2011-2080, April 2011.
[82] R.W. Gordon, J.J. Hollkamp, Coupled structural–acoustic response prediction with complex modal models, *Proceedings of the 50th Structures, Structural Dynamics and Materials Conference*, Palm Springs, California, AIAA-2009-2307, May 2009.